https://doi.org/10.5194/amt-2022-167
Preprint. Discussion started: 21 June 2022

Atmospheric Measurement Techniques Discussions

Direct measurement of N_2O_5 heterogeneous uptake coefficients on ambient aerosols via an aerosol flow tube system: design, characterization and performance

Xiaorui Chen[1,a], Haichao Wang[3,4*], Tianyu Zhai[1], Chunmeng Li[1], Keding Lu[1,2*]

[1]State Key Joint Laboratory of Environmental Simulation and Pollution Control, College of Environmental Sciences and Engineering, Peking University, Beijing, China.

[2]The State Environmental Protection Key Laboratory of Atmospheric Ozone Pollution Control, College of Environmental Sciences and Engineering, Peking University, Beijing, China

[3]School of Atmospheric Sciences, Sun Yat-sen University, Zhuhai, 519082, China

[4]Guangdong Provincial Observation and Research Station for Climate Environment and Air Quality Change in the Pearl River Estuary, Key Laboratory of Tropical Atmosphere-Ocean System, Ministry of Education, Southern Marine Science and Engineering Guangdong Laboratory (Zhuhai), Zhuhai, 519082, China

[a]now at: Department of Civil and Environmental Engineering, The Hong Kong Polytechnic University, Hong Kong, China

Correspondence to: Haichao Wang (wanghch27@mail.sysu.edu.cn), Keding Lu (k.lu@pku.edu.cn)

Abstract. An aerosol flow tube system coupled with detailed box model was newly developed to measure N_2O_5 heterogeneous uptake coefficients ($\gamma(N_2O_5)$) on ambient aerosols directly. This system features simultaneous measurements of N_2O_5 concentration at the both entrance and exit of the flow tube to ensure an accurate derivation of N_2O_5 loss in the flow tube. Simulation and laboratory tests demonstrate that this flow tube system is able to overcome the interference from side reactions led by varying reactants (e.g., NO_2, O_3 and NO) and improve the robustness of results with the assistance of box model method. Factors related to $\gamma(N_2O_5)$ derivation were extensively characterized, including particle transmission efficiency, mean residence time in the flow tube and wall loss coefficient of N_2O_5, for normal operating

https://doi.org/10.5194/amt-2022-167
Preprint. Discussion started: 21 June 2022


Atmospheric Measurement Techniques Discussions

condition. The measured $\gamma(N_2O_5)$ on $(NH_4)_2SO_4$ model aerosols were in good agreement with literature values over a range of relative humidity (RH). The detection limit of $\gamma(N_2O_5)$ was estimated to be 0.0016 at low aerosol surface concentration (Sa) condition of 200 μm^2 cm^{-3}. Given the instrument uncertainties and potential fluctuation of air mass between successive sampling modes, we estimate the overall uncertainty of $\gamma(N_2O_5)$ that ranges from 16 to 74% for different ambient conditions. This flow tube system was then successfully deployed for field observations at an urban site of Beijing influenced by anthropogenic emissions. The performance in field observation demonstrates that the current setup of this system is capable of obtaining robust $\gamma(N_2O_5)$ amid the switch of air mass.

1 Introduction

Dinitrogen pentoxide (N_2O_5), forming from the reaction of nitrogen dioxide (NO_2) and nitrate radical (NO_3), acts as an important reservoir of atmospheric nitrogen. The N_2O_5 can undergo either thermal dissociation (back to NO_2 and NO_3; photolysis of NO_3 also generate NO_2) to release NO_2 or hydrolysis (both homogeneous and heterogeneous) to remove nitrogen oxides from the atmosphere (Brown and Stutz, 2012;Chang et al., 2011). Among the budgets of N_2O_5, the uptake on aerosol particles is a highly efficient pathway to be responsible for production of nitrate aerosol in some regions (Fu et al., 2020;Wang et al., 2019;Wang et al., 2017c;Baasandorj et al., 2017;McDuffie et al., 2019;Prabhakar et al., 2017;Wang et al., 2018a;Chen et al., 2020) and promote activation of chlorine via $ClNO_2$ formation (Bertram and Thornton, 2009a;Osthoff et al., 2008;Tham et al., 2018;Thornton et al., 2010;Wang et al., 2017f). The N_2O_5 uptake coefficient ($\gamma(N_2O_5)$) is critical in determining the uptake reaction rate of N_2O_5 on aerosol in addition to aerosol surface area (Sa). It represents the fraction of collisions between gaseous N_2O_5 molecules and particle surfaces that resulted in a loss of N_2O_5. Model simulation showed the variations in $\gamma(N_2O_5)$ can significantly influence the fate of NOx, O_3 and OH radical in a regional (Li et al., 2016;Sarwar et al., 2012;Lowe et al., 2015) and global scale (Dentener and Crutzen, 1993;Evans and Jacob, 2005;Macintyre and Evans, 2010;Murray et al., 2021). However, ambient data of direct observation on $\gamma(N_2O_5)$ is still

https://doi.org/10.5194/amt-2022-167
Preprint. Discussion started: 21 June 2022


Atmospheric Measurement Techniques Discussions

scarce. It is thereby necessary to develop an accurate equipment or method to quantify this parameter on ambient aerosols.

Extensive laboratory experiments have been conducted to derive the values of $\gamma(N_2O_5)$ on aerosols and understand the mechanism of N_2O_5 uptake by various methods, including aerosol flow reactor (Kane et al., 2001;Mozurkewich and Calvert, 1988;Hu and Abbatt, 1997;Thornton and Abbatt, 2005;Thornton et al., 2003;Tang et al., 2014;Bertram and Thornton, 2009a), droplet train reactor (Van Doren et al., 1990;Schweitzer et al., 1998), Knudsen flow reactor (Karagulian et al., 2006) and smog chamber (Wahner et al., 1998;Wu et al., 2020). The $\gamma(N_2O_5)$ was found to be highly variable and dependent on particle chemical composition, acidity, phase state and the presence of organic coating using these laboratory methods under controllable conditions (Badger et al., 2006;Bertram et al., 2011;Fried et al., 1994;Griffiths et al., 2009;Gross et al., 2009;Hallquist et al., 2000;McNeill et al., 2006;Mentel et al., 1999;Riemer et al., 2003). While laboratory results have contributed to recognize the mechanism of N_2O_5 uptake and develop $\gamma(N_2O_5)$ parameterizations (Anttila et al., 2006;Bertram and Thornton, 2009b;Davis et al., 2008;Griffiths et al., 2009;Riemer et al., 2009), issues might emerge when quantitatively extended to ambient conditions due to the discrepancy between laboratory conditions and real air mass. For example, much higher reactant and particle concentration usually used in laboratory experiments might induce surface saturation or secondary reactions in a short time period, which lead to the bias of reaction rate used in ambient conditions. In addition, the physicochemical properties of ambient aerosol are much more complicated that the model aerosol used in laboratory studies, which led to the laboratory results on model aerosols are difficult to accurately represent what happens on the atmospheric aerosols.

There have been several methods implemented for field campaigns to indirectly derive $\gamma(N_2O_5)$, simply based on observation of ambient NO_3, N_2O_5, NO_2, O_3, $ClNO_2$, pNO_3^- and other auxiliary parameters without special equipment to capture the decay of N_2O_5 like laboratory ways. These include (1) the linear fit between N_2O_5 (NO_3) lifetime and the product of NO_2 and Sa concentration according to steady state equations (Brown et al., 2002;Brown et

https://doi.org/10.5194/amt-2022-167
Preprint. Discussion started: 21 June 2022


Atmospheric Measurement Techniques Discussions

al., 2009;Brown et al., 2006;Platt et al., 1984;Wang et al., 2017b;Wang et al., 2017d;Tham et al., 2016;Wang et al., 2017f;Brown et al., 2016), (2) the analysis of production rates of products (pNO_3^- and $ClNO_2$) resulting from N_2O_5 uptake under a stable condition (Mielke et al., 2013;Phillips et al., 2016;Wang et al., 2018b) and (3) box model simulations with an iterative approach to reproduce the evolutions of NO_3-N_2O_5 chemistry within each separate air mass after sunset (McDuffie et al., 2018;Wagner et al., 2013;Wang et al., 2020a;Yun et al., 2018). All these methods contain some specific assumptions and are only applicable in a few special cases.

To directly determine the $\gamma(N_2O_5)$ on ambient aerosols, Bertram et al. (2009a) firstly design an entrained aerosol flow reactor to adapt for low atmospheric Sa concentration with easy operation. By switching between filtered and bypass sampling mode, the N_2O_5 concentration at the exit of flow tube can be measured in the presence and absence of aerosols, respectively. The pseudo-first-order rate coefficients for N_2O_5 loss on aerosols is thereby derived from the ratio of measured N_2O_5 concentration in these two modes within a duty cycle according to Eq. 1:

$$k_{aerosols} = -\frac{1}{\Delta t}\ln\frac{[N_2O_5]_{\Delta t}^{w/particles}}{[N_2O_5]_{\Delta t}^{wo/particles}} \quad \text{Eq. 1}$$

where the Δt is the mean residence time of the flow tube, and the $[N_2O_5]_{\Delta t}^{wo/particles}$ and $[N_2O_5]_{\Delta t}^{w/particles}$ are the measured N_2O_5 concentration at the exit of flow tube in filtered and bypass mode, respectively. Assuming the gas-phase diffusion effect is negligible for atmospheric particles and low reaction probability (γ<0.1) (Fuchs and Sutugin, 1970), $\gamma(N_2O_5)$ can then be calculated from Eq. 2:

$$\gamma(N_2O_5) = \frac{4 \times k_{aerosols}}{c \times S_a} \quad \text{Eq. 2}$$

This method was deployed to measure $\gamma(N_2O_5)$ on ambient particles during two field campaigns (Bertram et al., 2009b;Riedel et al., 2012) and on aerosols generated in the laboratory (Ahern et al., 2018;Mitroo et al., 2019). While values of $\gamma(N_2O_5)$ were determined

https://doi.org/10.5194/amt-2022-167
Preprint. Discussion started: 21 June 2022


Atmospheric Measurement Techniques Discussions

to be robust in laboratory experiments, most of data would be dropped under ambient conditions due to the variations of wall loss coefficients (dominated by RH), fresh NO emission, N_2O_5 regeneration and flow pattern inside the flow tube. Based on the above measurement system, Wang et al. (2018c) added NOx, O_3 and Sa measurement on the exit of flow tube and introduce an iterative box model to minimize the potential influences from changing air mass and non-linear response of interference reactions. With the assumption of the equilibrium between NO_3 and N_2O_5, the box model runs backward and forward iteratively to obtain the N_2O_5 loss rate constant in the absence ($k_{het}^{wo/particles}$) and presence ($k_{het}^{w/particles}$) of aerosols respectively. The difference between these two parameters can finally derived the $\gamma(N_2O_5)$ according to Eq. 3, assuming the wall loss effect stays consistent.

$$\gamma(N_2O_5) = \frac{4(k_{het}^{w/particles} - k_{het}^{wo/particles})}{c \times S_a} \quad \text{Eq. 3}$$

This iterative approach was demonstrated to be able to buffer against certain fluctuations of air mass and measure $\gamma(N_2O_5)$ in the polluted atmosphere (Yu et al., 2020b).

Until now, only few direct measurements of $\gamma(N_2O_5)$ on ambient aerosols have been conducted during field campaigns (Bertram et al., 2009b;Riedel et al., 2012;Yu et al., 2020a). Even though combining with dataset from indirect approaches (e.g. steady state approximations), it is still challenging to characterize the temporal and spatial distributions of $\gamma(N_2O_5)$ on ambient aerosols. To better investigate the reactive uptake of N_2O_5 on aerosols in different environments, we develop an aerosol flow tube system with newly designed gas circuit and data acquisition procedures to quantify $\gamma(N_2O_5)$ on ambient aerosols. In the following sections, the setup of this system and laboratory characterizations for each part are described in details. Procedures of acquiring and processing data are compared to previous methods and discussed with potential uncertainties. Laboratory tests on model aerosols and field observations are presented to demonstrate its performance under varying ambient conditions.

https://doi.org/10.5194/amt-2022-167
Preprint. Discussion started: 21 June 2022

Atmospheric Measurement Techniques Discussions

2 The aerosol flow tube system

A schematic of the aerosol flow tube system is shown in Figure 1. The ambient air enters the system from the sampling manifold, mixes with gaseous N_2O_5 source in a Y-tee and flows to aerosol flow tube and detection instruments, as indicated by arrows in the figure. The system is distinct from previous flow tube systems due to its continuous monitor of NOx and O_3 concentration before the inlet of flow tube (after sampling air mixing with N_2O_5 source) and the simultaneous measurements of N_2O_5 concentration both at the inlet and the exit of flow tube within a duty cycle. Constraints of these variables during the subsequent data processing can enhance the measuring accuracy.

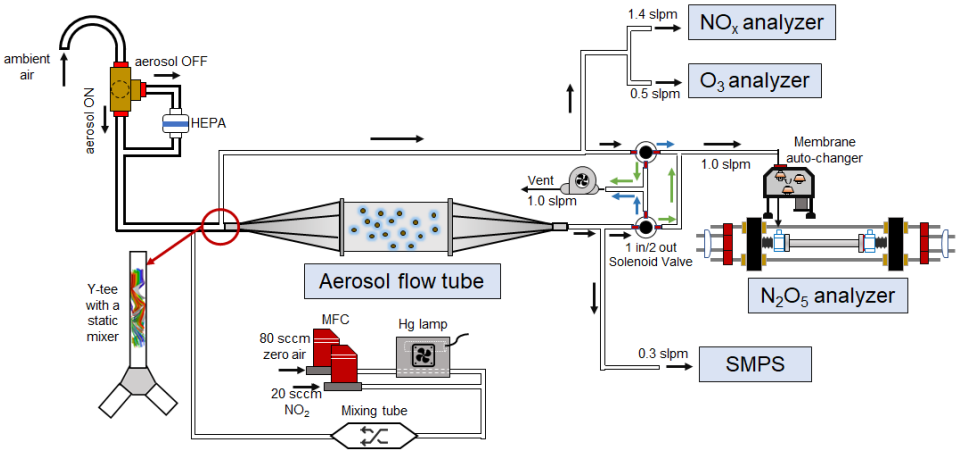

Figure 1. Overall schematic of aerosol flow tube system. The arrows alongside the tube show the flow directions. The black arrows indicate the flow directions consistent during the measurements, green arrows indicate the flow directions active in measuring the exit N_2O_5 and blue arrows indicate the flow directions active in measuring the inlet N_2O_5.

2.1 Sampling manifold

The sampling tube is made of a 50 cm long and half inch outside diameter (OD) aluminum tubing, with a curve tip (10 cm radius of curvature) turning the inlet straight down in order to avoid precipitation. The ambient air is then pass through a three-way solenoid ball valve, which is controlled by a time relay to either allow the air to flow directly into a following Y-

https://doi.org/10.5194/amt-2022-167
Preprint. Discussion started: 21 June 2022


Atmospheric Measurement Techniques Discussions

tee (filter bypass mode) or divert to a HEPA (high efficiency particulate air filter, Whatman) to remove particles (filter inline mode). We choose a stainless-steel ball valve with the same OD as the sampling tube to minimize the particle loss in filter bypass mode. The HEPA can retain particles at a high efficiency (>99.9%) with low pressure drop and RH difference between filter inline and bypass mode.

2.2 Gaseous N_2O_5 generation

A home-made temperature-controlled gas generator is used to generate gaseous N_2O_5 in-situ via the reaction of O_3 with NO_2 (R1) and the subsequent reaction of produced NO_3 with NO_2 (R2).

$$NO_2 + O_3 \rightarrow NO_3 + O_2 \qquad \text{R1}$$

$$NO_2 + NO_3 + M \leftrightarrow N_2O_5 + M \qquad \text{R2}$$

NO_2 is delivered from a compressed gas cylinder (20 ppmv in N_2 diluent gas, Jinghao Corp.). O_3 is generated from the photolysis of O_2 in compressed ultra-pure synthetic zero air at 254 nm, using a commercial mercury lamp (UVP, the USA) fixed inside the generator. The produced O_3 are then mixed with NO_2 in a small darkened Teflon reaction tube for about 2 min under the temperature of 15 ℃, stabilized by a Peltier cooler controlled by a proportion integration differentiation algorithm. A PFA tube with polyethylene foam was used to transmit the synthesized N_2O_5 to sampling stream and minimize the influence of ambient temperature variation on N_2O_5 level. The flow rate of NO_2 (20 sccm) and zero air (80 sccm) are controlled by mass flow controller separately at a total of 100 sccm. By changing the flow rate ratio between NO_2 and zero air, the generator can produce N_2O_5 concentration varying from 1 ppbv to 6 ppbv (after dilution in zero air at sampling flow rate of 4.5 slpm). Under the typical measurement condition, an excess of NO_2 concentration is applied to shift the equilibrium towards N_2O_5 production (R2) and suppress the NO_3 concentration to less than 30 pptv, which is expected to decrease the uncertainty of varying NO_3 reactivity (NO, VOCs and heterogeneous loss). The resulted initial N_2O_5 concentration was 4.0 ppbv at the inlet of aerosol flow tube, together with around 50 ppbv of NO_2 and 15 ppbv of O_3. A stability test on

https://doi.org/10.5194/amt-2022-167
Preprint. Discussion started: 21 June 2022


Atmospheric Measurement Techniques Discussions

N_2O_5 source showed the variation was within 1% for a 24-h continuous operation, with ambient temperature ranging from 0 to 15 °C.

2.3 Aerosol flow tube

Air flow enters and exits the flow tube via two identical conical diffuser caps at a diffuser angle of 45°. A 35cm×14 cm inner diameter (ID) cylindrical tube is mounted in the middle of two caps, flanged with screws and nitrile rubber O-rings. All sections of this aerosol flow tube are made of stainless-steel with electro-polished and FEP-coated inside. The exterior of the flow tube is insulated with aluminum coated polyethylene foam 3 cm thick to minimize thermal eddies fluctuation of ambient temperature. Under the typical flow rate of 2.1 SLPM in the flow tube, the axial velocity in the cylindrical tube section is 0.23 $cm \cdot s^{-1}$ which produces a Reynolds numbers (*Re*) of 22, well below the threshold of laminar flow (*Re*<2100).

In front of the flow tube, the synthesized N_2O_5 source is introduced perpendicular to ambient air sampling stream via a regular stainless-steel tee and then the mixture enters a stainless-steel Y-tee for further mixing. The inner surface of both regular tee and Y-tee is electro-polished and coated with SilcoNert 2000 (Silotek Corp.), a technique commonly applied in semiconductor industry, to maintain the transmission efficiency of particles and minimize the loss of N_2O_5 in the meantime. A 10 cm long stainless-steel static mixer is mounted inside the Y-tee in order to swirl the flow and thus facilitate the mixing between sampling stream and N_2O_5 source in a relatively short distance. The presence of static mixer at the inlet also help to improve the flow expansion performance after entering the flow tube by minimizing flow recirculating towards the wall, which decreases the wall loss of N_2O_5 and particles (Huang et al., 2017). After passing through the static mixer, the mixture of ambient air and N_2O_5 source is split into two flows at the same flow rate, one of which straightly enters the aerosol flow tube and the other one is diverted to measurements of NOx, O_3 and N_2O_5. We measured the concentrations of NOx, O_3, N_2O_5 and Sa at the both exits of Y-tee under typical flow rate for three repeated experiments (Figure 2). Almost the same gaseous concentrations and particle distributions at both exits of Y-tee demonstrate that the N_2O_5 source has been well mixed with the sampling flow and species concentrations at the inlet of flow tube can be

https://doi.org/10.5194/amt-2022-167
Preprint. Discussion started: 21 June 2022

Atmospheric Measurement Techniques Discussions

202 accurately determined via the measurements at the other exit of Y-tee.

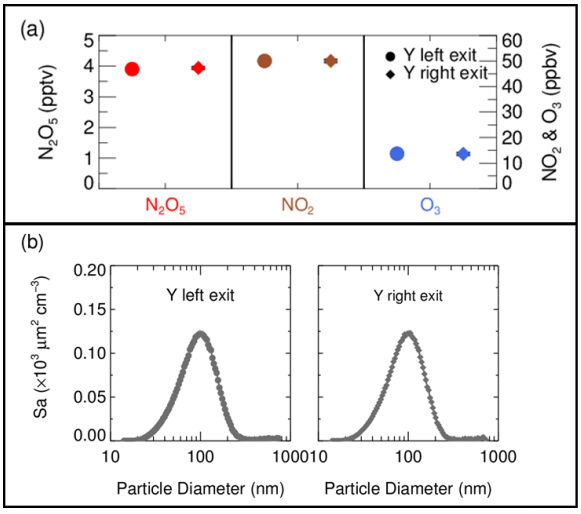

203

204 **Figure 2.** (a) The concentration of N_2O_5, NO_2 and O_3 in the mixture of N_2O_5 source and
205 sampling aerosols measured at each exit of Y-tee; (b) The size distribution of Sa concentration
206 in the mixture of N_2O_5 gas source and sampling aerosols measured at each exit of Y-tee.

207 ## 2.4 Detection instruments

208 Instruments used in this system are listed in Table 1. A portable cavity-enhanced absorption
209 spectrometer (CEAS) is used to measure N_2O_5 concentration (Wang et al., 2017a) at both inlet
210 and exit of the aerosol flow tube by automatically switching the flow directions (see details in
211 section 2.5). Briefly, the N_2O_5 is thermally decomposed to NO_3 by heating up to 130℃ and
212 then quantified according to the extinction coefficient caused by NO_3 absorption in the
213 wavelength window from 640 to 680 nm. A Teflon polytetrafluoroethylene (PTFE) membrane
214 is placed in front of the CEAS to remove particles, which will be replaced with a new one
215 every two hours by a self-designed membrane auto-changer. Laboratory tests have been
216 conducted to quantified the transmission efficiency of N_2O_5 over the membrane (92±3%),
217 sampling tube of CEAS (99.7%) and the inside of CEAS (93.6%). The detection limit of N_2O_5
218 was determined to be 2.7 pptv (1σ, 60s) and the measurement uncertainty was 19%. A time-
219 resolution of 60 s for N_2O_5 data acquisition is typically used to derive $\gamma(N_2O_5)$ in this study.
220 The CEAS has been successfully applied to measure ambient N_2O_5 concentration in several

https://doi.org/10.5194/amt-2022-167
Preprint. Discussion started: 21 June 2022


Atmospheric Measurement Techniques Discussions

field campaigns and laboratory studies (Chen et al., 2020;Wang et al., 2020a;Wang et al., 2017b;Wang et al., 2020b;Wang et al., 2018b;Wang et al., 2022).

Table 1. Performance of related instruments incorporated in the flow tube system.

Parameter	Technique	Time resolution	Detection Limit(1σ)	Accuracy
NO	Chemiluminescence[a]	1 min	200 pptv	±10%
NO_2	Chemiluminescence	1 min	300 pptv	±10%
O_3	UV photometry	1 min	500 pptv	±5%
VOCs	GC-MS/FID[b]	60 min	20-300 pptv	±15%
N_2O_5	CEAS	1 min	2.7 pptv	±19%
Sa	SMPS	5 min	-	±10%
RH&T	Sensor	1 min	-	±0.1%&±0.1K

[a] Photolytic conversion to NO through blue light before detection; [b] Gas chromatography equipped with a mass spectrometer and a flame ionization detector;

At the inlet of flow tube, NOx concentration is measured via chemiluminescence method equipped with a blue-light photolytic converter (Thermo, Model 42i) and O_3 concentration is also measured via chemiluminescence method by adding excessive NO (Teledyne API, Model T265). Both NOx and O_3 concentration are averaged to 1 min time-resolution. The size distribution of particle number density is measured at the exit of flow tube using a scanning mobility particle sizer (SMPS, TSI 3776), which determines the total Sa concentration covering the range from 13 to 730 nm. Particles larger than this range usually contributed less than 5% of total Sa according to our previous field measurements (Chen et al., 2020) and it is included in the uncertainty analysis (see section 5). A cycle of size scanning is set to around 5 min and the derived Sa concentration is then interpolated into 1 min for further calculation. Aerosols pass through a Nafion tubing (MD-700) before entering into SMPS to reduce RH to less than 30%. The dry-state Sa is therefore corrected to wet-state at the RH inside the flow tube for particle hygroscopicity. The growth factor, $f(RH)=1+8.77\times(RH/100)^{9.74}$, used for correction is valid only when RH is within the range from 30 to 90% (Liu et al., 2013). The RH and temperature of flow are continuously measured both before entering and after leaving the flow tube by commercial sensors (Rotronic, Model HC2A-S). The averages of the values

https://doi.org/10.5194/amt-2022-167
Preprint. Discussion started: 21 June 2022


Atmospheric Measurement Techniques Discussions

obtained at both locations are used to represent the RH and temperature inside the flow tube. In addition, ambient volatile organic compounds (VOCs) are measured in-situ alongside the aerosol flow tube system using an online gas chromatograph mass spectrometer coupled with a flame ionization detector (GCMS-FID) to derive the NO_3 reactivity to VOCs ($k_{NO3\text{-}VOCs}$) in the flow tube.

2.5 Procedures of data acquisition

The N_2O_5 concentration is acquired at both inlet and exit of the flow tube within a duty cycle via a CEAS instrument, which is different from that only at the exit of the flow tube in previous studies (Bertram et al., 2009a;Wang et al., 2018c). At each duty cycle, consisting of once HEPA inline mode for measuring k_{wall} of N_2O_5 and once HEPA bypass mode for retrieving the N_2O_5 loss on aerosols, the procedure that measuring N_2O_5 at the inlet of flow tube followed by that at the exit is executed twice with one for each mode. An exemplary case obtained during a field campaign is shown in Figure 3 to explain this procedure. Within the mode of HEPA inline, N_2O_5 data is firstly acquired at the inlet of the flow tube and then switch to the exit of the flow tube. The $k_{het}^{wo/particles}$, which is the k_{wall} of N_2O_5, can be therefore derived from a box model constrained by these N_2O_5 data (see section 3 for the model description and data processing). The same procedures are executed in the mode of HEPA bypass, except the $\gamma(N_2O_5)$ is derived according to Eq 2. Two three-way valves controlled by a time relay were implemented to realize this procedure in order to avoid the changes of flow condition in the flow tube that could have been caused. As indicated in Figure 1, the blue arrows show the flow directions when measuring the N_2O_5 concentration at the inlet of flow tube, while the green arrows shows that for the exit of flow tube. It should be noted that the concentration of NOx and O_3 are always acquired at the inlet of the flow tube and the Sa concentration always at the exit of the flow tube during the operation.

https://doi.org/10.5194/amt-2022-167
Preprint. Discussion started: 21 June 2022

Atmospheric Measurement Techniques Discussions

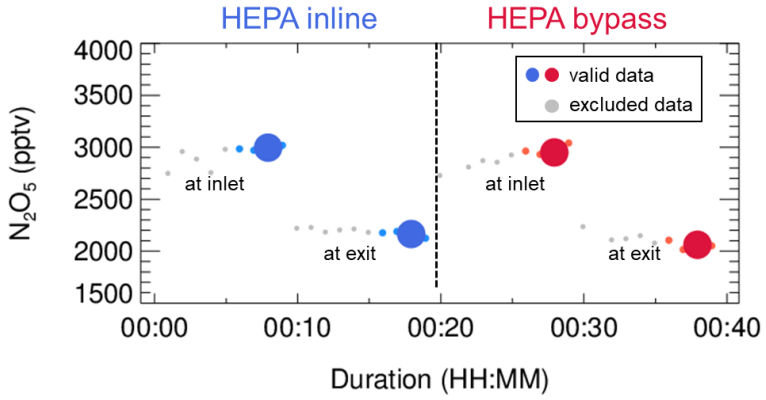

Figure 3. An exemplary case of measured N_2O_5 concentration within a duty cycle. This case was observed on the night of 13 December 2020, with average ambient Sa of 320 μm^2 cm^{-3}. The derived k_{wall} of N_2O_5 and $\gamma(N_2O_5)$ were 0.0023 s^{-1} and 0.035, respectively. The blue dots indicate N_2O_5 concentration measured under the mode of HEPA inline either at the inlet or exit of the flow tube (denoted as texts); the respective averages (blue dots of larger size) are used for deriving k_{wall} (blue square). The red dots indicate N_2O_5 concentration measured under the mode of HEPA bypass either at the inlet or exit of the flow tube; the respective averages (red dots of larger size) are used for deriving the overall rate constant of N_2O_5 loss on the wall and aerosols. The data points in gray are excluded from calculation due to unstable conditions in the flow tube.

In addition, laboratory tests were conducted to determine a suited duration for each duty cycle. During a duty cycle, the duration for each mode should last long enough to develop a stable flow condition for particles or empty particles, while a much longer duration could decrease the measurement time-resolution and leads to large uncertainty due to the fluctuations within a long time period. We measured Sa and N_2O_5 concentration continuously at the exit of flow tube when sampling $(NH_4)_2SO_4$ aerosols. As shown in Figure 4, it took about 15 minutes for particles to rise to a stable level from none or to decrease from a certain level to none, when our system underwent mode switches. The correspondingly periodical variation of N_2O_5 concentration was consistent with particles. The residence time distribution (RTD) profiles (see in section 4.2) also demonstrated that it required at least 10 minutes for gaseous species to evolve to a stable condition after a mode switch. As a result, a typical duration of duty cycle is determined to be 40 minutes with 20 minutes for each mode. The N_2O_5 measurement at the

https://doi.org/10.5194/amt-2022-167
Preprint. Discussion started: 21 June 2022

Atmospheric Measurement Techniques Discussions

289 exit of the flow tube in the last 5 minutes of each mode is able to represent valid decays of
290 N_2O_5 under this mode and satisfy the requirements of further data processing.

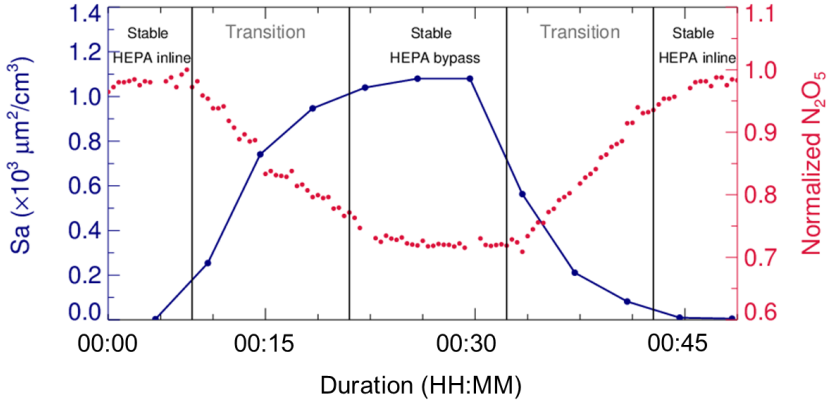

291

292 **Figure 4.** Variations of Sa and N_2O_5 concentration (normalized to peak values) measured at
293 the exit of flow tube when switching the sampling mode. The phases of species concentrations
294 in the flow tube approaching stable after a mode switch are denoted as the transition phases.

295 ## 3 Box model for determination of loss rate coefficients of N_2O_5

296 ### 3.1 Method description

297 Large uncertainties were found in retrieving $\gamma(N_2O_5)$ on ambient particles according to Eq. 1
298 in a previous flow tube study (Bertram et al., 2009a), due to the dependence of homogeneous
299 reaction rates on sampling modes and the atmospheric variations of parameters related to NO_3-
300 N_2O_5 chemistry (e.g. NO, NO_2, O_3, VOCs, and RH). To minimize these influences, a time-
301 dependent box model constrained by the measurements of N_2O_5 concentration and other
302 auxiliary parameters is applied to calculate loss rate coefficients of N_2O_5 under the mode of
303 HEPA inline and bypass, respectively. The model is able to simulate the reactions related to
304 budgets of NO_3-N_2O_5 chemistry in a dark condition, including R1, R2 and the follows:

$$NO_3 + NO \rightarrow 2\ NO_2 \qquad \text{R3}$$

$$NO_3 + VOCs \rightarrow products \qquad \text{R4}$$

https://doi.org/10.5194/amt-2022-167
Preprint. Discussion started: 21 June 2022


Atmospheric Measurement Techniques Discussions

N_2O_5 + aerosols or wall → products R5

The rate constants for reactions R1 to R3 are referenced to IUPAC database. The reaction of VOCs and NO_3 is treated as pseudo-first-order with a rate constant of $k_{NO3\text{-}VOCs}$, which is calculated from the sum of rate constants for reactions of NO_3 with each VOCs scaled by the concentration of VOCs measured by GC-FID. Due to low time-resolution of VOCs measurements (1 h), the $k_{NO3\text{-}VOCs}$ is kept constant for each derivation of $\gamma(N_2O_5)$. The suppressed NO_3 concentration is expected to attenuate the influence resulted from the uncertainty of $k_{NO3\text{-}VOCs}$ (see discussion in section 5). The reaction R5 represents the loss of N_2O_5 only on the wall in the mode of HEPA inline or on the both wall and particles in the mode of HEPA bypass. The rate constant of R5 is also treated as pseudo-first-order and it is adjustable among different runs.

The same procedures of data screening and model operation are applied to both sampling and bypass modes, as shown in Figure 5. For example, in the mode of HEPA inline, the average of NO concentration less than 6 ppbv and the variation of N_2O_5 measured at the inlet of flow tube less than 10% should be validated prior to the following model operation. Under typical concentration of N_2O_5 source we used in this flow tube system, the exit concentration of N_2O_5 is detected to be under triple detection limit with initial NO large than 6 ppbv according to our laboratory tests. In ambient condition, high level of NO is usually also accompanied by rapid variation due to fresh emission, which disturbs the decay of N_2O_5 in the flow tube and leads to large uncertainty in deriving its loss rate coefficient. Excluding the cases that N_2O_5 measured at the inlet of flow tube varies exceeding 10% can further minimize the uncertainty of N_2O_5 loss rate coefficient resulted from rapid change of NO_3 reactants (NO, VOCs). If the measured data within the duration of a sampling mode satisfies the criteria for data screening described above, the model can therefore simulate the reactions starting from the entrance of flow tube and lasting for 156 s (mean residence time) based on these data. The initial concentrations of $[NO]_{t=0}$, $[NO_2]_{t=0}$, $[O_3]_{t=0}$ and $[N_2O_5]_{t=0}$ are the averages of last-5-min values measured at the inlet of flow tube. The RH and temperature are constrained by the mean values during this sampling mode. By tuning the loss rate coefficient of N_2O_5 (k_{N2O5}) in the way of

https://doi.org/10.5194/amt-2022-167
Preprint. Discussion started: 21 June 2022

Atmospheric Measurement Techniques Discussions

binary search, we optimized an appropriate k_{N2O5} to ensure that the N_2O_5 concentration output from the simulation is consistent with last-5-min average of N_2O_5 concentration measured at the exit of flow tube within 1 pptv. As a result, this derived k_{N2O5} (aka. $k_{het}^{wo/particles}$) is expected to be the k_{wall} of N_2O_5. The same procedures above are then applied to the data obtained in the mode of HEPA bypass, except that the derived k_{N2O5} (aka. $k_{het}^{w/particles}$) contains the loss rate coefficients of N_2O_5 on the both wall and particles. It should be noted that the above calculation for obtained data is only valid under the variation of RH less than 2% within a duty cycle and the k_{wall} of N_2O_5 can then be reasonably assumed to be constant between two successive sampling modes. Therefore, the $\gamma(N_2O_5)$ can be retrieved by the Eq 3, where the last-5-min averages of Sa concentration in the mode of HEPA bypass is used.

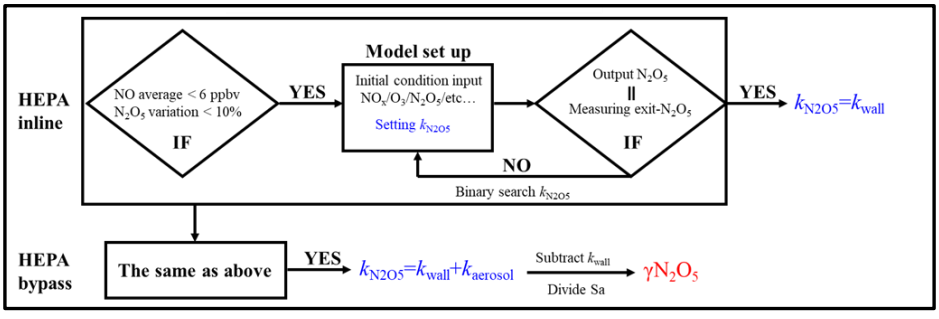

Figure 5. Flow diagram of $\gamma(N_2O_5)$ derivation through box model method.

3.2 Evaluation of the box model method

The box model method is introduced to our flow tube system in order to overcome the influence from homogeneous reactions and variations of air mass on $\gamma(N_2O_5)$ derivation. A series of scenarios were provided to evaluate the performance of box model method under these influences. We allow NO, NO_2 and O_3 in the mixture of sampling air at the entrance of the flow tube to vary in a reasonable range, in order to set up the scenarios of different gradients of NO concentration and NO_3 production rates (PNO_3). Other relevant parameters were prescribed to be fixed, including N_2O_5 source of 4 ppbv, Sa concentration of 1000 $\mu m^2 \cdot cm^{-3}$, $\gamma(N_2O_5)$ of 0.02, k_{wall} of 0.002 s^{-1}, $k_{NO3\text{-}VOCs}$ of 0.01 s^{-1} and temperature 298K. By simulating N_2O_5 evolutions in the flow tube based on these conditions, the exit concentration of N_2O_5

https://doi.org/10.5194/amt-2022-167
Preprint. Discussion started: 21 June 2022


Atmospheric Measurement Techniques Discussions

with and without particles will be obtained for various scenarios. The $\gamma(N_2O_5)$ on particles are then calculated according to Eq 1&2 or by box model method used in this study. Comparison between the results of two methods indicates that the box model method is more robust in retrieving $\gamma(N_2O_5)$ due to the consideration of multiple reactions in the flow tube.

As shown in Figure 6(a), the exit concentration method ($\gamma(N_2O_5)$ exit-conc., derived directly by Eqs. 1-2) underestimates $\gamma(N_2O_5)$ by varying degrees at different levels of PNO_3, while the box model method can well reproduce the same $\gamma(N_2O_5)$ implemented in these simulations (not shown). The PNO_3 is calculated from the initial NO_2 and O_3 concentration. The degree of this underestimation for exit concentration method is mainly related to the in situ N_2O_5 production in the flow tube. With a sustaining production of NO_3 via the reaction of NO_2 to O_3 and rapid heterogeneous loss of N_2O_5 in the flow tube, the equilibrium between NO_3 and N_2O_5 always shifts to the production of N_2O_5, and masking the actual amount of N_2O_5 removal. In the mode of HEPA bypass, the N_2O_5 consumes faster than the other mode due to the addition of particles, which further facilitates the N_2O_5 formation through the equilibrium. Therefore, more N_2O_5 produced with particles in the flow tube leads to the underestimation of $\gamma(N_2O_5)$ calculated by the exit concentration method. The increase of PNO_3 contributes to amplify this underestimation up to around 60% at a relatively polluted environment, which could be encountered in southern China even during the wintertime. Previous studies also found similar impacts from N_2O_5 production on retrieving $\gamma(N_2O_5)$ in the aerosol flow tube (Bertram et al., 2009a;Wang et al., 2018c). In addition, the discrepancy of $\gamma(N_2O_5)$ derived by two methods is much less dependent on the NO concentration at least in the prescribed range of NO. As the ratio of NO_3/N_2O_5 is relatively small (<1%) in our N_2O_5 source, the difference of NO titration rates between two sampling modes has little impact on N_2O_5 concentration and the subsequent $\gamma(N_2O_5)$ derivation.

To corroborate the results of comparison predicted by simulations, we also performed laboratory tests to measure $\gamma(N_2O_5)$ on $(NH_4)_2SO_4$ aerosols using our flow tube system under typical operating condition. The aerosols were conditioned to RH of 50% and doped with NO gas (10 ppmv in N_2 diluent gas, Jinghao Corp.) at different gradients by diluted in ultrahigh-

https://doi.org/10.5194/amt-2022-167
Preprint. Discussion started: 21 June 2022

Atmospheric Measurement Techniques Discussions

purity N_2. Figure 6(b) shows that the $\gamma(N_2O_5)$ derived by box model method is at 0.01 and consistent over the range of NO concentration from 0 to 6 ppbv applied to the tests. This result agrees well with previous laboratory observation of $\gamma(N_2O_5)$ on $(NH_4)_2SO_4$ aerosols within uncertainty (Badger et al., 2006;Hallquist et al., 2003;Kane et al., 2001). Similar to simulation tests, the exit concentration method again underestimates $\gamma(N_2O_5)$ by 50 to 60% in the laboratory tests, which reinforces that it is necessary for $\gamma(N_2O_5)$ measurements by an aerosol flow tube to consider the interactions between homogeneous and heterogeneous reactions in the flow tube using the box mode method especially with a long residence time. The absence of dependence between NO concentration and $\gamma(N_2O_5)$ results also provides us the confidence that this aerosol flow tube system is able to buffer against NO within the range from 0 to 6 ppbv under typical operating condition. However, this is not always the case when the NO is accompanied with rapid fluctuations in a real atmosphere, which might lead to intractable uncertainty and is therefore excluded from further analysis according to the criteria of data screening described above.

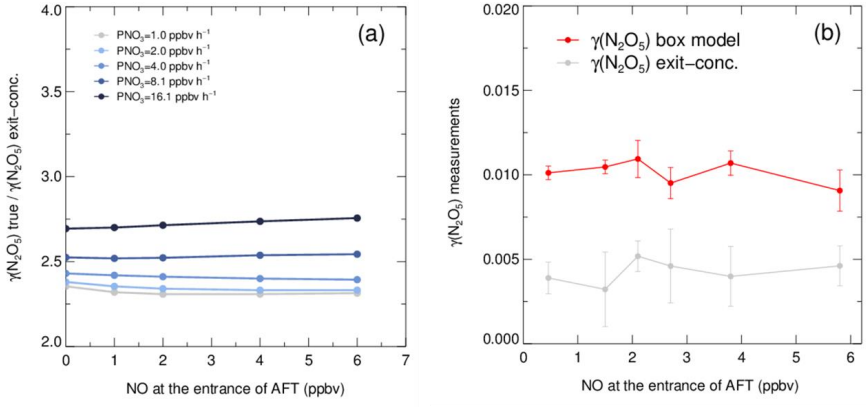

Figure 6. Simulated and laboratory tests on performance of box model method and exit concentration method for $\gamma(N_2O_5)$ derivation. (a) The ratios of given $\gamma(N_2O_5)$ ($\gamma(N_2O_5)$ true) over exit concentration derived $\gamma(N_2O_5)$ ($\gamma(N_2O_5)$ exit-conc.) determined from simulated scenarios. The $\gamma(N_2O_5)$ derived by box model method is exactly the same as $\gamma(N_2O_5)$ true. The ratios vary with NO concentration and the lines are color coded by PNO_3 values. Both NO concentration and PNO_3 represent the values at the entrance of aerosol flow tube. (b) $\gamma(N_2O_5)$ measurements on lab-generated $(NH_4)_2SO_4$ aerosols under different gradients of NO with

https://doi.org/10.5194/amt-2022-167
Preprint. Discussion started: 21 June 2022


Atmospheric Measurement Techniques Discussions

constant RH of 50% and PNO_3 typically generated from our N_2O_5 source. The red line shows the $\gamma(N_2O_5)$ derived by box model method and gray line shows the $\gamma(N_2O_5)$ derived by exit concentration method. The NO concentrations are measured at the entrance of aerosol flow tube.

Overall, the introduction of box model method in this study is able to effectively avoid the underestimation caused by the lack of consideration of side reactions in the flow tube. Although an iterative box model, including backward and forward simulation, has been successfully applied to realize the $\gamma(N_2O_5)$ measurements via an aerosol flow tube in polluted environments (Wang et al., 2018c), the box model method combined with current flow tube system in this study can improve measuring accuracy on some aspects. First, we simulate NO_3-N_2O_5 relationship via specific reactions rather than approximating it in equilibrium and introducing the equilibrium coefficient (*K*eq) into calculation. Determining NO_3 or N_2O_5 concentration by *K*eq could induce large bias under the high aerosol loading and low temperature (Chen et al., 2021). Second, it is more accurate to constrain the box model with directly measured NOx, O_3 and N_2O_5 at the entrance of the flow tube. Under a real atmosphere, the initial N_2O_5 concentration after mixing with sampling air is expected to be not as stable as that observed in laboratory tests, due to the variations in temperature, NO concentration and other related parameters. Numerical simulations based on a constant initial N_2O_5 and estimation of initial concentrations for other species through backward simulation could then lead to bias in the resulting $\gamma(N_2O_5)$ under these conditions.

4 Laboratory characterizations

4.1 Particle transmission efficiency

The transmission efficiency of particles in the sampling module and flow tube are estimated respectively in Figure 7. In the laboratory, pure ammonia nitrate ($(NH_4)_2SO_4$) aerosols were generated from an atomizer loading with 0.1 M $(NH_4)_2SO_4$ solution. The RH and concentration of produced aerosols flow was conditioned in a glass bottle (~2 L) by introducing a humidified dilution flow of ultrahigh-purity N_2. As a result, aerosols in different concentrations

https://doi.org/10.5194/amt-2022-167
Preprint. Discussion started: 21 June 2022

Atmospheric Measurement Techniques Discussions

(1000~4500 μm^2 cm^{-3}) and under a range of RH (20~70%) were applied to test the transmission efficiency. Figure 7(a) shows the loss of total Sa concentration in the sampling module and flow tube are 8±1% and 10±2% on average, respectively. We found that the fraction of particles loss is mainly caused by particles smaller than 100 nm. This is most likely due to the turbulence generated by static mixer and the recirculation in the flow tube. Large particles are prone to stay within the main flow direction, whereas small particles readily adsorb on the walls by the entrainment of turbulence or recirculation. In addition, the particles distribution measured at the exit of flow tube with HEPA inline (gray line in Figure 7(a)) demonstrated its capability of removing almost all particles (>99.5%) at the typical flow rate. Transmission efficiency tests were also conducted on ambient aerosols (Figure 7(b)) and the resulted loss of total Sa concentration was similar to that using laboratory-generated aerosols.

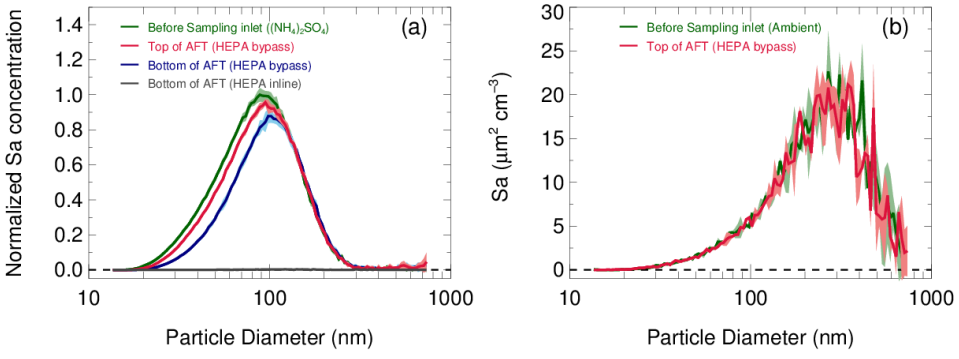

Figure 7. (a) Particles transmission determined by sampling laboratory-generated $(NH_4)_2SO_4$ aerosols. Aerosols at different concentrations and RH levels are used in experiments and the size distribution of Sa concentration are normalized to the peak values. The normalized size distribution of Sa concentration measured before sampling inlet (green line), at the inlet of flow tube with HEPA bypass (red line) and at the bottom of flow tube with HEPA bypass (blue line) are shown respectively. Under the mode of HEPA inline, the Sa concentration was almost zero at the bottom of flow tube (gray line). The shadows indicate the standard deviations of the normalized Sa concentration for all experiments. (b) Particles transmission determined by sampling ambient particles.

4.2 Residence time in the flow tube

The method of residence time distribution (RTD) was applied to estimate the average reaction

https://doi.org/10.5194/amt-2022-167
Preprint. Discussion started: 21 June 2022


Atmospheric Measurement Techniques Discussions

time of the gas species in the flow tube (residence time). In comparison to ideal plug flow, the RTD method can better describe actual behavior of the flow in practice and determine the mean residence time more accurately (Danckwerts, 1953). Several studies have also used this RTD method to determine the residence time in the flow tube (Huang et al., 2017;Wang et al., 2018c;Lambe et al., 2011).

The RTD profiles were obtained by introducing a 2 s pulse of NO_2 gas diluted in N_2 into the flow tube under RH less than 1%. NO_2 is relatively inert against the flow tube wall coated with FEP and was measured at the exit of the flow tube by a CEAS (Li et al., 2021) at high time-resolution (2 Hz). A three-way solenoid valve combined with a time relay was implemented to control the pulse in order to avoid the disturbance on flow condition from the injection. Experiments were performed under typical operation. The mean residence time (t_{ave}) can be derived from the each RTD profile according to Eq. 4,

$$t_{ave} = \frac{\sum_{i=0} C_i \times t_i}{\sum_{i=0} C_i}, \quad \text{Eq. 4}$$

where the C_i is the concentration of NO_2 recorded at the time step t_i. From the RTD profiles of NO_2 injection experiments in Figure 8, the determined t_{ave} was 156±3 s. This value is 19% less than the space time (τ_{space}, flow tube volume divided by operation flow rate, 192.6 s). It has also been found that the assumption of ideal plug flow overestimated the residence time in previous flow tube experiments (Lambe et al., 2011;Huang et al., 2017;Wang et al., 2018c), which could lead to underestimation of the derived k_{N2O5}.

https://doi.org/10.5194/amt-2022-167
Preprint. Discussion started: 21 June 2022

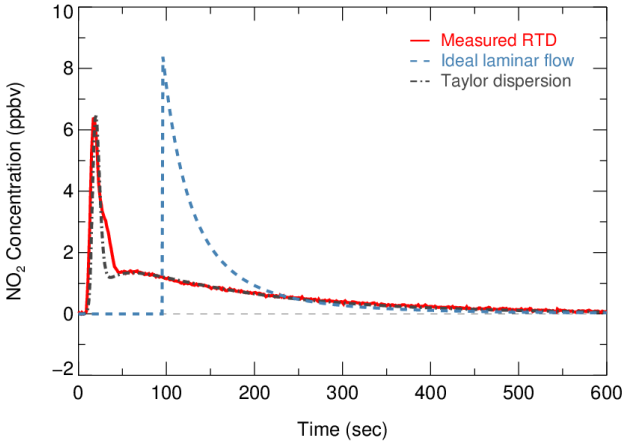

Figure 8. Residence time distribution derived by sampling NO_2 gas. Red solid line indicates the measured RTD profiles. The calculated RTD of ideal laminar flow (without dispersions) and the Taylor dispersion model fitted to measurements are shown as blue dash line and dot-dash line, respectively.

Two theoretical RTDs were calculated, namely ideal laminar flow and Taylor diffusion, besides the measured RTD, intending to reflect the fluid field inside the flow tube. The ideal laminar flow describes the flow without dispersion. The velocity profile of ideal laminar flow is parabolic, with the fluid in the center of the tube moving the fastest. According to the following Eq. 5, the RTD of ideal laminar flow is scaled by the integrated concentration of NO_2 and presented as the blue dash line in Figure 8.

$$\begin{cases} 0, & t < 0.5\tau_{space} \\ \dfrac{{\tau_{space}}^2}{2t^3}, & t \geq 0.5\tau_{space} \end{cases}, \qquad \text{Eq. 5}$$

While the determined *Re* is well within the laminar flow threshold, the measured RTD occurs earlier than theoretical laminar flow condition and exhibits a broaden distribution. The discrepancy between them indicates that the dispersions or potential secondary flows could dominate the flow regime. Instead, an improved Taylor dispersion model (shown as the gray dot-dash line in Figure 8) is able to reproduce the measured RTD, which was previously implemented in the characterization of photooxidation flow reactors (Lambe et al., 2011). Two flow patterns with distinct effective diffusivities (0.02 and 0.51 derived from best fit) were

https://doi.org/10.5194/amt-2022-167
Preprint. Discussion started: 21 June 2022

Atmospheric Measurement Techniques Discussions

490 considered in this dispersion model. An implication from the characteristics of the model is
491 that two flow components consist of the flow regime: a direct flow path through the flow tube
492 with less diffusion and a secondary flow path representing the recirculation in the dead zone
493 that induced by temperature gradient and significant diffusions (Huang et al., 2017).

494 **4.3 N_2O_5 wall loss**

495 The stainless-steel flow tube in this study is electro-polished and coated by FEP inside to
496 reduce the loss of N_2O_5 and particles on the wall in the meantime. An electro-polished surface
497 could enhance the homogeneity of FEP-coating and reduce the adsorption of H_2O molecule to
498 the wall, which influences the loss of N_2O_5. It has been found that the k_{wall} of N_2O_5 increases
499 with the RH (Bertram et al., 2009a;Wang et al., 2018c). Therefore, a less change in k_{wall} of
500 N_2O_5 from RH helps to minimize the uncertainty induced by fluctuations of RH within a duty
501 cycle. Laboratory tests were conducted to quantify the k_{wall} of N_2O_5 under different levels of
502 RH with HEPA inline. As shown in Figure 9, the k_{wall} of N_2O_5 gradually increase from 0.002
503 s^{-1} in a dry condition to 0.006 s^{-1} when RH is 70%. The level of k_{wall} is less than the result of
504 Wang et al. (2018c) but higher than Bertram et al. (2009a) as indicated in Table 2. In addition,
505 the flow tube was rinsed with deionized water every week during the field campaigns to
506 remove the build-up of particles, which might increase the hygroscopicity of the internal
507 surface and thus the k_{wall} of N_2O_5 in a wet condition. Uncertainty in $\gamma(N_2O_5)$ derivation resulted
508 from the variation of k_{wall} related to RH is discussed in section 5.

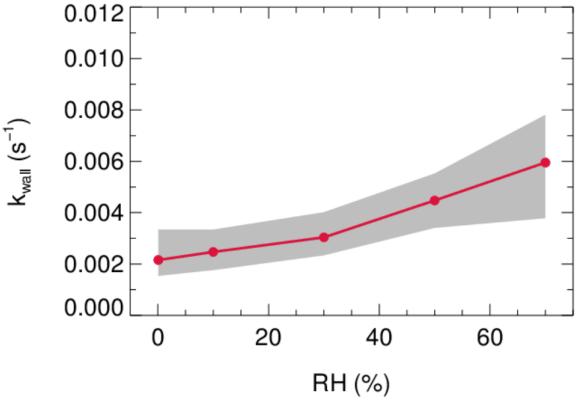

509

510 **Figure 9**. The dependence of pseudo-first-order wall loss coefficient (k_{wall}) of N_2O_5 in the

https://doi.org/10.5194/amt-2022-167
Preprint. Discussion started: 21 June 2022


Atmospheric Measurement Techniques Discussions

FEP-coated aerosol flow tube.

Table 2. Summary of the k_{wall} of N_2O_5 for the existing aerosol flow tube deployed in field campaigns.

RH range	k_{wall} range ($\times 10^{-3}$ s^{-1})	References
5~50%	0.5~3	Bertram et al., 2009
20~70%	4~9	Wang et al., 2018
0~70%	2~6	This work

4.4 Demonstration of $\gamma(N_2O_5)$ measurements on model particles

$\gamma(N_2O_5)$ measurements by current aerosol flow tube system equipped with box model method were performed on lab-generated $(NH_4)_2SO_4$ aerosols over a range of RH. The system was operated at room temperature of 295K with N_2O_5 concentration of 4.0 ppbv at the entrance of flow tube. We conditioned the RH of generated aerosols by introducing dry N_2 gas dilution, which could decrease the RH level down to 10~55%, starting from over 95% where $(NH_4)_2SO_4$ aerosols are expected to be in aqueous state. The resulting Sa concentrations of aerosols were around 600 $\mu m^2 \cdot cm^{-3}$. As shown in Figure 10, the observed $\gamma(N_2O_5)$ values were below 0.01 when RH was within 40% and significantly rose up to 0.02 with higher RH. The dependence of $\gamma(N_2O_5)$ on RH and the exact values are well consistent with previous laboratory results on $(NH_4)_2SO_4$ aerosols (Badger et al., 2006;Hallquist et al., 2003;Hu and Abbatt, 1997;Kane et al., 2001;Mozurkewich and Calvert, 1988), which shows that the setup of our instrument has good practicability. A large standard deviation of $\gamma(N_2O_5)$ found at RH of 39% is possibly due to the unstable phase transition of $(NH_4)_2SO_4$ particles, as its efflorescence RH is reportedly from 35 to 48% (Martin, 2000).

https://doi.org/10.5194/amt-2022-167
Preprint. Discussion started: 21 June 2022

Atmospheric Measurement Techniques Discussions

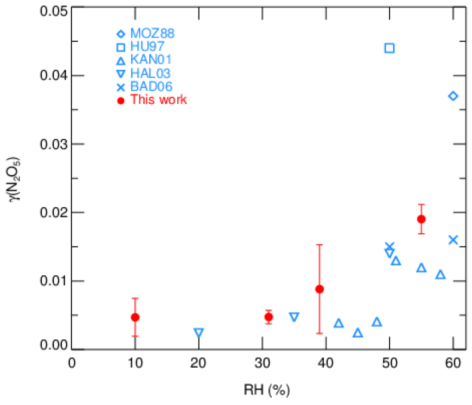

Figure 10. The dependence of $\gamma(N_2O_5)$ on RH for laboratory-generated $(NH_4)_2SO_4$ aerosols. The red points with standard deviations represent the values measured by current aerosol flow tube system in this work. Previously reported values are indicated in blue marks.

5 Uncertainty analysis and detection limit

The uncertainty of $\gamma(N_2O_5)$ is in relevance to the measurement uncertainties of each instrument and rapid fluctuations of various parameters. As outlined before, the 5-min averages of N_2O_5 concentration measured at the inlet and exit of the flow tube were used for calculating $\gamma(N_2O_5)$ via the box model method. The potential variations within these selected time periods would therefore lead to relative errors. For example, the variations of N_2O_5 concentration is resulted majorly from the rapid changes of ambient NO and less from variations of VOCs, NO_2, O_3 as well as N_2O_5 gas source itself (1% in 24 hours). A cutoff of 10% for N_2O_5 variation was implemented to filter out the air mass that was too unstable for valid analysis, according to our prescribed criteria of data screening. It consequently leads to 10% uncertainty in the average of N_2O_5 and can translate into a deviation of 2% in $\gamma(N_2O_5)$ with the $\gamma(N_2O_5)$ at 0.02, Sa at 800 $\mu m^2 \cdot cm^{-3}$ and other parameters (shown in Table 3) representing the typical inlet values measured during the field campaign (described in section 6). Similarly, cases that over 2% variation in RH exists between the HEPA inline and bypass mode are excluded from analysis, owing to its significant influence on k_{wall} of N_2O_5 in the flow tube. By assuming a consistent k_{wall} in successive sampling modes, the potential variations in RH could lead to uncertainty in

https://doi.org/10.5194/amt-2022-167
Preprint. Discussion started: 21 June 2022


Atmospheric Measurement Techniques Discussions

549 $\gamma(N_2O_5)$ from $\pm 8 \times 10^{-4}$ at RH of 20% to $\pm 2 \times 10^{-3}$ at RH of 70%, respectively, with the Sa at
550 800 μm^2 cm^{-3}. In addition, the $k_{NO3\text{-}VOCs}$ is treated as constant in a duty cycle due to the limit
551 of time resolution of VOCs measurements. A variation of ± 0.01 s^{-1} in $k_{NO3\text{-}VOCs}$ only induces
552 less than ±1% uncertainty in $\gamma(N_2O_5)$ for more than 95% cases obtained during the field
553 campaign. All the impacts from inherent instruments uncertainties and variations of different
554 parameters are thereby considered in Monte Carlo simulations to assess the overall uncertainty
555 of $\gamma(N_2O_5)$. The basic simulation is initialized with the typical conditions measured at the inlet
556 of the flow tube during the field campaign and repeatedly performs the procedures of
557 determining $\gamma(N_2O_5)$ via the box model method 1000 times. In each run, all parameters were
558 allowed to vary independently within a prescribed range, presented in Table 3.

559 **Table 3.** Parameters involved in the Monte Carlo simulations.

Parameters	Value [a]	Variation range [b]
NO	1 ppbv	±10%
NO_2	70 ppbv	±10%
O_3	10 ppbv	±5%
Inlet N_2O_5	4 ppbv	±19%
Exit N_2O_5 [c]	2.2 ppbv	±19%
Temperature	273 K	±0.1 K
RH [d]	30 %	±1%
$k_{NO3\text{-}VOCs}$	0.01 s^{-1}	±0.01 s^{-1}

560 [a] Values used for initializing Monte Carlo simulations in a basic scenario; [b] Ranges within
561 which each parameter can vary independently; [c] Determined from the case that $\gamma(N_2O_5)$ is at
562 0.02, Sa is at 800 $\mu m^2 \cdot cm^{-3}$ and other parameters are shown in this table; [d] The RH and its
563 variation can be transformed into values in k_{wall} of N_2O_5 via the fitting function derived from
564 Figure 9.

565 The resulting $\gamma(N_2O_5)$ values from Monte Carlo simulations under the basic scenario are
566 shown as frequency distributions in Figure 11(a). This distribution can be fitted by a Gaussian
567 function and the standard deviation (1σ) of Gaussian distribution is regarded as the overall

https://doi.org/10.5194/amt-2022-167
Preprint. Discussion started: 21 June 2022


Atmospheric Measurement Techniques Discussions

568 uncertainty of $\gamma(N_2O_5)$, which is $\pm 9 \times 10^{-4}$ (4.5% relative to true $\gamma(N_2O_5)$). The uncertainty of
569 Sa measurements and unmeasured particles larger than 730 nm (usually less than 5% of total
570 Sa) would together introduce an extra 16% uncertainty to $\gamma(N_2O_5)$.

571 We further found that the uncertainty of $\gamma(N_2O_5)$ could be sensitive to the measurement
572 conditions. With higher O_3, potential variations of NO and $k_{NO3\text{-}VOCs}$ will induce larger
573 uncertainty of $\gamma(N_2O_5)$ (Figure 11(b)), as it enhances the abundance of NO_3 and N_2O_5. In
574 comparison, the low O_3 in the basic scenario suppressed the side formation of NO_3 in the flow
575 tube, limiting the aggravation of $\gamma(N_2O_5)$ uncertainty from the increase of NO and NO_2. The
576 $\gamma(N_2O_5)$ uncertainty is also positive correlated with RH and T. As is discussed before, the k_{wall}
577 of N_2O_5 increases with RH level, which can amplify the potential bias of k_{wall} at a higher RH
578 level. The equilibrium between NO_3 and N_2O_5 shifts towards the decomposition of N_2O_5 at
579 higher T, leading to larger uncertainty of $\gamma(N_2O_5)$ caused by potential variations of NO and
580 $k_{NO3\text{-}VOCs}$. The overall uncertainty of $\gamma(N_2O_5)$ therefore rises to 8.2% at the RH of 70% and to
581 14.4% at the temperature of 293K (Figure 11(c)), with NO, NO_2, O_3, $\gamma(N_2O_5)$ and Sa keeping
582 the same as the basic scenario. In addition, Monte Carlo simulations were also performed for
583 different $\gamma(N_2O_5)$ values ranging from 0.01 to 0.08. The uncertainty of $\gamma(N_2O_5)$ clearly
584 decreased with the $\gamma(N_2O_5)$ (Figure 11(d)). A lower $\gamma(N_2O_5)$ weaken the impacts N_2O_5 uptakes
585 has on the budgets of NO_3 and N_2O_5, which causes the $\gamma(N_2O_5)$ derivation to be more
586 susceptible to uncertainties of other parameters and then increases the uncertainty of $\gamma(N_2O_5)$.

https://doi.org/10.5194/amt-2022-167
Preprint. Discussion started: 21 June 2022

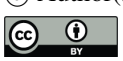

Atmospheric Measurement Techniques Discussions

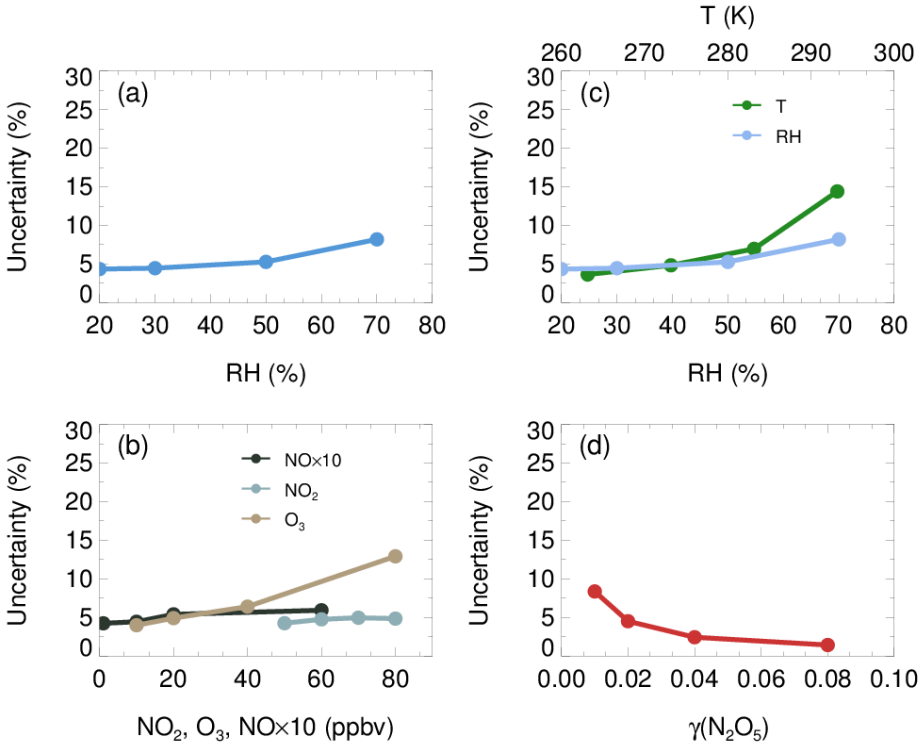

Figure 11. The uncertainty of $\gamma(N_2O_5)$ determined from the Monte Carlo simulations. (a) Histogram distribution of $\gamma(N_2O_5)$ generated from a Monte Carlo simulation (1000 single runs) in the basic scenario (shown as Table 2), where the overall uncertainty of $\gamma(N_2O_5)$ was determined to be $\pm 9\times10^{-4}$; (b) dependence of the uncertainty of $\gamma(N_2O_5)$ on NO, NO_2 as well as O_3; (c) dependence of the uncertainty of $\gamma(N_2O_5)$ on RH and T; (d) dependence of the $\gamma(N_2O_5)$ uncertainty on $\gamma(N_2O_5)$ level.

In addition, the mean residence time used in the box model method could bias the retrieved $\gamma(N_2O_5)$ due to the non-normal distribution of residence time with a discernable tail. The reactants entrained by those slower streamlines close to the wall will take much longer time to reach the exit of the flow tube than that by the centerline. In order to evaluate the uncertainty caused by the distribution of residence time, we first performed simulations of N_2O_5 decay in the flow tube under the basic scenarios and calculate the exit N_2O_5 concentration according to the probability distribution function derived from RTD profile. Then the $\gamma(N_2O_5)$ can be retrieved from the box model method running for the duration of mean residence time,

https://doi.org/10.5194/amt-2022-167
Preprint. Discussion started: 21 June 2022

Atmospheric Measurement Techniques Discussions

602 constrained by this calculated exit N_2O_5 concentration. The result shows an underestimation
603 of $\gamma(N_2O_5)$ derived from the mean residence time reaching 32% in the basic scenario. The
604 extent of underestimation is most sensitive to the level of $\gamma(N_2O_5)$ and RH. In short, when
605 taking all the factors and their corresponding varying ranges discussed above into
606 consideration, the overall uncertainty of $\gamma(N_2O_5)$ determined from Monte Carlo simulations is
607 in the range of 16-74%.

608 In order to determine the detection limit of the current aerosol tube system, the continuous
609 blank measurements in zero air were performed with settled operation procedures. Within per
610 duty cycle (40 minutes), one k_{wall} of N_2O_5 and one $\gamma(N_2O_5)$ can be derived in pair. In total, we
611 obtained 56 sets of result. The detection limit of k_{N2O5} on aerosols is 2.1×10^{-5} s^{-1}, derived from
612 1σ of the Gaussian function fitted to this distribution. It is equivalent to 0.0016 for the detection
613 limit of $\gamma(N_2O_5)$ with a low Sa condition of 200 μm^2 cm^{-3} (Figure 12(a)), and 0.00064 for the
614 detection limit of $\gamma(N_2O_5)$ with a moderate Sa condition of 500 μm^2 cm^{-3} (Figure 12(b)). This
615 result indicates that the flow tube system has capability of quantifying $\gamma(N_2O_5)$ for most cases
616 even under a low aerosol-loading environment.

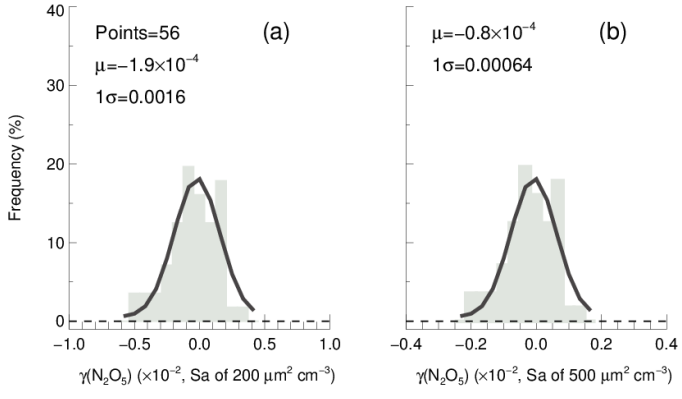

617

618 **Figure 12**. The $\gamma(N_2O_5)$ derived from blank measurements in histogram distribution plot. The
619 $\gamma(N_2O_5)$ was calculated from k_{N2O5} by Eq 2 with Sa of (a) 200 μm^2 cm^{-3} and (b) 500 μm^2 cm^{-3},
620 respectively, under the temperature of 293K. The Gaussian function is fitted to the distribution
621 and plotted in black line. The 1σ from Gaussian fit is regarded as the detection limit.

https://doi.org/10.5194/amt-2022-167
Preprint. Discussion started: 21 June 2022


Atmospheric Measurement Techniques Discussions

6 Performance in the field campaign

The aerosol flow tube system was successfully deployed to measure $\gamma(N_2O_5)$ on ambient aerosols in Beijing lasting for 20 days during the December of 2020. The sampling site was at the campus of Peking University, which is located in the city center of Beijing surrounded by major roads with heavy traffic. Therefore, this site represents an area with large amount of fresh emission of NOx and other anthropogenic sources. The system was mounted in the top floor of a building, about 15 m height above the ground. The sampling manifold was placed in open air and the ambient aerosols could directly enter the inlet of the manifold without additional sampling tubes. During the period of measurement, the averages of ambient temperature, RH, NO, NO_2, O_3 and Sa were 273 ± 3 K, 25 ± 12 %, 23 ± 36 ppbv, 23 ± 12 ppbv, 16 ± 15 ppbv and 409 ± 249 μm^2 cm^{-3}, respectively. The NO and Sa levels could vary by 2 orders of magnitude due to the periodical switch between clean air mass from the north and pollutants accumulated by local emission.

A total of 99 valid $\gamma(N_2O_5)$ values were determined from the measurements based on the criteria of data screening described in section 3.1. We found that $\gamma(N_2O_5)$ was 0.042±0.026 on average with a median of 0.035, ranging from 0.0045 to 0.12 (Figure 13). These results are comparable to that previously determined in the North of China using various different methods (Wang et al., 2017b;Wang et al., 2018b;Wang et al., 2017d;Wang et al., 2017e;Xia et al., 2019;Yu et al., 2020a). The k_{wall} of N_2O_5 corresponding to valid $\gamma(N_2O_5)$ measurements was rather stable at an average of 0.0021±0.0007 s^{-1}, which was consistent with the values determined at similar RH levels in the laboratory tests. It somehow reflected the robustness of the status of the flow tube system and the derived results.

In the current system, the N_2O_5 concentrations measured at both entrance and exit of the flow tube are sensitive to the NO fluctuations within the timescale of one sampling mode, which can induce large uncertainty on calculating $\gamma(N_2O_5)$. With our stringent criteria of data screening, the cases of drastic NO fluctuations were excluded from the analysis. Hence, the majority of valid $\gamma(N_2O_5)$ for this campaign were obtained during the periods of the NO below 2 ppbv, when the clean air mass was dominant at this urban site. Meanwhile, the Sa

https://doi.org/10.5194/amt-2022-167
Preprint. Discussion started: 21 June 2022

Atmospheric Measurement Techniques Discussions

concentration within clean episodes were also lower than other periods, with an average of 159 μm^2 cm^{-3}. The derived k_{N2O5} ranged from 2.1×10^{-5} to 1.6×10^{-3} s^{-1} well above the detection limit, which demonstrated the robustness of results even subject to low ambient Sa conditions. In order to improve the applicability of $\gamma(N_2O_5)$ measurements, future development is suggested to prioritize the reduction or removal of NO level (at least the fluctuation of NO) in the sampling system before the entrance of flow tube without the cost of particles transmission efficiency.

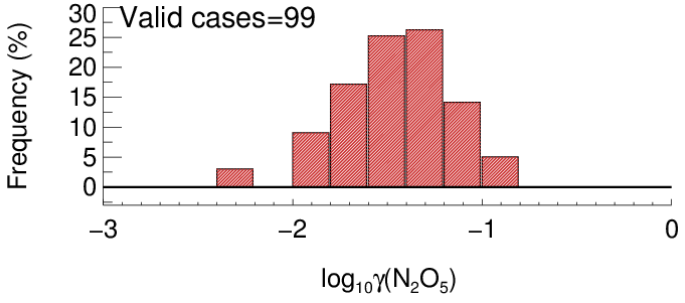

Figure 13. The histogram distribution of measured $\gamma(N_2O_5)$ for valid cases.

7 Summary and conclusion

We report a new development of an aerosol flow tube system coupled with detailed box model to derive $\gamma(N_2O_5)$ directly on ambient aerosols. The unique feature of this system is that the simultaneous N_2O_5 measurement at the both ends of flow tube was applied to improve the accuracy in quantifying $\gamma(N_2O_5)$, by taking it as a constraint for the box model to reproduce the decay of introduced N_2O_5 gas source in the flow tube. With the consideration of detailed chemistry related to N_2O_5, the proposed approach was testified to refrain from the interference of side reactions under different conditions, induced by the additional N_2O_5 generation, NO titration in the flow tube and variations of air masses between successive sampling modes.

A series of laboratory tests were performed to characterize factors affecting $\gamma(N_2O_5)$ derivation and demonstrate its applicability on $(NH_4)_2SO_4$ aerosols. The uncertainties associated with instruments used in the system and potential fluctuations of various parameters were thoroughly discussed in the uncertainty analysis, and we estimated the overall uncertainty

https://doi.org/10.5194/amt-2022-167
Preprint. Discussion started: 21 June 2022


Atmospheric Measurement Techniques Discussions

of $\gamma(N_2O_5)$ to be 16-74% which is subject to NO, NO_2, O_3, meteorological parameters, residence time and $\gamma(N_2O_5)$ value itself. The detection limit of $\gamma(N_2O_5)$ was quantified to be 0.0016 at the aerosol surface concentration (Sa) of 200 μm^2 cm^{-3}. We deployed this system for field observations of $\gamma(N_2O_5)$ at an urban site in Beijing, where strong anthropogenic emission and periodically switch of air mass were encountered. The obtained $\gamma(N_2O_5)$ was in comparable level to previously reported values in the north of China and demonstrated the robustness of this system within low NO episodes. Further investigations on N_2O_5 heterogeneous chemistry for both laboratory-generated and ambient particles are also available by the introduced approach.

https://doi.org/10.5194/amt-2022-167
Preprint. Discussion started: 21 June 2022


Atmospheric Measurement Techniques Discussions

682 **Code/Data availability.** The datasets used in this study are available from the corresponding
683 author upon request (wanghch27@mail.sysu.edu.cn; k.lu@pku.edu.cn).
684
685 **Author contributions.** K.D.L. and H.C.W. designed the study. X.R.C and H.C.W. analyzed
686 the data and wrote the paper with input from K.D.L.
687
688 **Competing interests**. The authors declare that they have no conflicts of interest.
689
690 **Acknowledgments**. This project is supported by the National Natural Science Foundation of
691 China (21976006, 42175111); the Beijing Municipal Natural Science Foundation for
692 Distinguished Young Scholars (JQ19031); National State Environmental Protection Key
693 Laboratory of Formation and Prevention of Urban Air Pollution Complex (CX2020080578);
694 the special fund of the State Key Joint Laboratory of Environment Simulation and Pollution
695 Control (21K02ESPCP); the National Research Program for Key Issue in Air Pollution
696 Control (DQGG0103-01, 2019YFC0214800). Thanks for the data contributed by field
697 campaign team.
698

699 **References**

700 Ahern, A. T., Goldberger, L., Jahl, L., Thornton, J., and Sullivan, R. C.: Production of N_2O_5 and $ClNO_2$ through
701 Nocturnal Processing of Biomass-Burning Aerosol, Environmental Science & Technology, 52, 550-559,
702 10.1021/acs.est.7b04386, 2018.
703 Anttila, T., Kiendler-Scharr, A., Tillmann, R., and Mentel, T. F.: On the reactive uptake of gaseous compounds
704 by organic-coated aqueous aerosols: Theoretical analysis and application to the heterogeneous hydrolysis of N_2O_5,
705 J. Phys. Chem. A, 110, 10435-10443, 10.1021/jp062403c, 2006.
706 Baasandorj, M., Hoch, S. W., Bares, R., Lin, J. C., Brown, S. S., Millet, D. B., Martin, R., Kelly, K., Zarzana, K.
707 J., Whiteman, C. D., Dube, W. P., Tonnesen, G., Jaramillo, I. C., and Sohl, J.: Coupling between Chemical and
708 Meteorological Processes under Persistent Cold-Air Pool Conditions: Evolution of Wintertime PM2.5 Pollution
709 Events and N_2O_5 Observations in Utah's Salt Lake Valley, Environmental Science & Technology, 51, 5941-5950,
710 10.1021/acs.est.6b06603, 2017.
711 Badger, C. L., Griffiths, P. T., George, I., Abbatt, J. P. D., and Cox, R. A.: Reactive uptake of N_2O_5 by aerosol
712 particles containing mixtures of humic acid and ammonium sulfate, J. Phys. Chem. A, 110, 6986-6994,

https://doi.org/10.5194/amt-2022-167
Preprint. Discussion started: 21 June 2022


Atmospheric Measurement Techniques Discussions

713 10.1021/jp0562678, 2006.
714 Bertram, A. K., Martin, S. T., Hanna, S. J., Smith, M. L., Bodsworth, A., Chen, Q., Kuwata, M., Liu, A., You, Y.,
715 and Zorn, S. R.: Predicting the relative humidities of liquid-liquid phase separation, efflorescence, and
716 deliquescence of mixed particles of ammonium sulfate, organic material, and water using the organic-to-sulfate
717 mass ratio of the particle and the oxygen-to-carbon elemental ratio of the organic component, Atmos. Chem.
718 Phys., 11, 10995-11006, 10.5194/acp-11-10995-2011, 2011.
719 Bertram, T., and Thornton, J.: Toward a general parameterization of N 2 O 5 reactivity on aqueous particles: the
720 competing effects of particle liquid water, nitrate and chloride, Atmos. Chem. Phys., 9, 8351-8363, 2009a.
721 Bertram, T. H., and Thornton, J. A.: Toward a general parameterization of N_2O_5 reactivity on aqueous particles:
722 the competing effects of particle liquid water, nitrate and chloride, Atmos. Chem. Phys., 9, 8351-8363,
723 10.5194/acp-9-8351-2009, 2009b.
724 Bertram, T. H., Thornton, J. A., and Riedel, T. P.: An experimental technique for the direct measurement of N_2O_5
725 reactivity on ambient particles, Atmospheric Measurement Techniques, 2, 231-242, 10.5194/amt-2-231-2009,
726 2009a.
727 Bertram, T. H., Thornton, J. A., Riedel, T. P., Middlebrook, A. M., Bahreini, R., Bates, T. S., Quinn, P. K., and
728 Coffman, D. J.: Direct observations of N_2O_5 reactivity on ambient aerosol particles, Geophys. Res. Lett., 36,
729 10.1029/2009gl040248, 2009b.
730 Brown, S., Stark, H., Ciciora, S., McLaughlin, R., and Ravishankara, A. R.: Simultaneous in situ Detection of
731 Atmospheric NO_3 and N_2O_5 via Cavity Ring-down Spectroscopy, Rev. Sci. Instrum., 73, 3291-3301,
732 10.1063/1.1499214, 2002.
733 Brown, S. S., Ryerson, T. B., Wollny, A. G., Brock, C. A., Peltier, R., Sullivan, A. P., Weber, R. J., Dube, W. P.,
734 Trainer, M., Meagher, J. F., Fehsenfeld, F. C., and Ravishankara, A. R.: Variability in nocturnal nitrogen oxide
735 processing and its role in regional air quality, Science, 311, 67-70, 10.1126/science.1120120, 2006.
736 Brown, S. S., Dube, W. P., Fuchs, H., Ryerson, T. B., Wollny, A. G., Brock, C. A., Bahreini, R., Middlebrook, A.
737 M., Neuman, J. A., Atlas, E., Roberts, J. M., Osthoff, H. D., Trainer, M., Fehsenfeld, F. C., and Ravishankara, A.
738 R.: Reactive uptake coefficients for N_2O_5 determined from aircraft measurements during the Second Texas Air
739 Quality Study: Comparison to current model parameterizations, J. Geophys. Res.- Atmos., 114, D00F10(01-16),
740 Artn D00f10
741 10.1029/2008jd011679, 2009.
742 Brown, S. S., and Stutz, J.: Nighttime radical observations and chemistry, Chem. Soc. Rev., 41, 6405-6447,
743 10.1039/c2cs35181a, 2012.
744 Brown, S. S., Dubé, W. P., Tham, Y. J., Zha, Q., Xue, L., Poon, S., Wang, Z., Blake, D. R., Tsui, W., Parrish, D.
745 D., and Wang, T.: Nighttime chemistry at a high altitude site above Hong Kong, J. Geophys. Res.: Atmos., 121,
746 2457-2475, 10.1002/2015jd024566, 2016.
747 Chang, W. L., Bhave, P. V., Brown, S. S., Riemer, N., Stutz, J., and Dabdub, D.: Heterogeneous atmospheric
748 chemistry, ambient measurements, and model calculations of N_2O_5: A review, Aerosol Sci. Technol., 45, 665-695,
749 2011.
750 Chen, X., Wang, H., Lu, K., Li, C., Zhai, T., Tan, Z., Ma, X., Yang, X., Liu, Y., Chen, S., Dong, H., Li, X., Wu,
751 Z., Hu, M., Zeng, L., and Zhang, Y.: Field Determination of Nitrate Formation Pathway in Winter Beijing,
752 Environmental Science & Technology, 54, 9243-9253, 10.1021/acs.est.0c00972, 2020.
753 Chen, X., Wang, H., and Lu, K.: Interpretation of NO 3–N 2 O 5 observation via steady state in high aerosol air
754 mass: The impact of equilibrium coefficient in ambient conditions, Atmospheric Chemistry and Physics

https://doi.org/10.5194/amt-2022-167
Preprint. Discussion started: 21 June 2022

755 Discussions, 1-14, 2021.
756 Danckwerts, P. V.: Continuous flow systems: distribution of residence times, Chem. Eng. Sci., 2, 1-13, 1953.
757 Davis, J. M., Bhave, P. V., and Foley, K. M.: Parameterization of N_2O_5 reaction probabilities on the surface of
758 particles containing ammonium, sulfate, and nitrate, Atmos. Chem. Phys., 8, 5295-5311, 10.5194/acp-8-5295-
759 2008, 2008.
760 Dentener, F. J., and Crutzen, P. J.: Reaction Of N_2O_5 On Tropospheric Aerosols - Impact On The Global
761 Distributions Of NOx, O_3, And OH, Journal of Geophysical Research Atmospheres, 98, 7149-7163, 1993.
762 Evans, M., and Jacob, D. J.: Impact of new laboratory studies of N_2O_5 hydrolysis on global model budgets of
763 tropospheric nitrogen oxides, ozone, and OH, Geophys. Res. Lett., 32, 2005.
764 Fried, A., Henry, B. E., Calvert, J. G., and Mozurkewich, M.: THE REACTION PROBABILITY OF N_2O_5 WITH
765 SULFURIC-ACID AEROSOLS AT STRATOSPHERIC TEMPERATURES AND COMPOSITIONS, J.
766 Geophys. Res.- Atmos., 99, 3517-3532, 10.1029/93jd01907, 1994.
767 Fu, X., Wang, T., Gao, J., Wang, P., Liu, Y., Wang, S., Zhao, B., and Xue, L.: Persistent Heavy Winter Nitrate
768 Pollution Driven by Increased Photochemical Oxidants in Northern China, Environ. Sci. Technol., 54, 3881-3889,
769 10.1021/acs.est.9b07248, 2020.
770 Fuchs, N. A., and Sutugin, A. G.: Highly Dispersed Aerosol, Halsted Press, 1970.
771 Griffiths, P. T., Badger, C. L., Cox, R. A., Folkers, M., Henk, H. H., and Mentel, T. F.: Reactive Uptake of N_2O_5
772 by Aerosols Containing Dicarboxylic Acids. Effect of Particle Phase, Composition, and Nitrate Content, J. Phys.
773 Chem. A, 113, 5082-5090, 10.1021/jp8096814, 2009.
774 Gross, S., Iannone, R., Xiao, S., and Bertram, A. K.: Reactive uptake studies of NO_3 and N_2O_5 on alkenoic acid,
775 alkanoate, and polyalcohol substrates to probe nighttime aerosol chemistry, PCCP, 11, 7792-7803,
776 10.1039/b904741g, 2009.
777 Hallquist, M., Stewart, D. J., Baker, J., and Cox, R. A.: Hydrolysis of N_2O_5 on submicron sulfuric acid aerosols,
778 J. Phys. Chem. A, 104, 3984-3990, 10.1021/jp9939625, 2000.
779 Hallquist, M., Stewart, D. J., Stephenson, S. K., and Anthony Cox, R.: Hydrolysis of N_2O_5 on sub-micron sulfate
780 aerosols, PCCP, 5, 3453, 10.1039/b301827j, 2003.
781 Hu, J. H., and Abbatt, J. P. D.: Reaction probabilities for N_2O_5 hydrolysis on sulfuric acid and ammonium sulfate
782 aerosols at room temperature, J. Phys. Chem. A, 101, 871-878, DOI 10.1021/jp9627436, 1997.
783 Huang, Y., Coggon, M., Zhao, R., Lignell, H., Bauer, M., Flagan, R., and Seinfeld, J.: The Caltech Photooxidation
784 Flow Tube reactor: Design, fluid dynamics and characterization, Atmospheric Measurement Techniques, 10, 839-
785 867, 10.5194/amt-10-839-2017, 2017.
786 Kane, S. M., Caloz, F., and Leu, M. T.: Heterogeneous uptake of gaseous N_2O_5 by $(NH_4)_2SO_4$, NH_4HSO_4, and
787 H_2SO_4 aerosols, J. Phys. Chem. A, 105, 6465-6470, 10.1021/jp010490x, 2001.
788 Karagulian, F., Santschi, C., and Rossi, M.: The heterogeneous chemical kinetics of N 2 O 5 on CaCO 3 and
789 other atmospheric mineral dust surrogates, Atmos. Chem. Phys., 6, 1373-1388, 2006.
790 Lambe, A., Ahern, A., Williams, L., Slowik, J., Wong, J., Abbatt, J., Brune, W., Ng, N., Wright, J., and Croasdale,
791 D.: Characterization of aerosol photooxidation flow reactors: heterogeneous oxidation, secondary organic aerosol
792 formation and cloud condensation nuclei activity measurements, Atmospheric Measurement Techniques, 4, 445-
793 461, 2011.
794 Li, C. M., Wang, H. C., Chen, X. R., Zhai, T. Y., Chen, S. Y., Li, X., Zeng, L. M., and Lu, K. D.: Thermal
795 dissociation cavity-enhanced absorption spectrometer for measuring NO_2, RO_2NO_2, and $RONO_2$ in the
796 atmosphere, Atmospheric Measurement Techniques, 14, 4033-4051, 10.5194/amt-14-4033-2021, 2021.

https://doi.org/10.5194/amt-2022-167
Preprint. Discussion started: 21 June 2022

Li, Q., Zhang, L., Wang, T., Tham, Y. J., Ahmadov, R., Xue, L., Zhang, Q., and Zheng, J.: Impacts of heterogeneous uptake of dinitrogen pentoxide and chlorine activation on ozone and reactive nitrogen partitioning: improvement and application of the WRF-Chem model in southern China, Atmos. Chem. Phys., 16, 14875-14890, 10.5194/acp-16-14875-2016, 2016.

Liu, X., Gu, J., Li, Y., Cheng, Y., Qu, Y., Han, T., Wang, J., Tian, H., Chen, J., and Zhang, Y.: Increase of aerosol scattering by hygroscopic growth: Observation, modeling, and implications on visibility, Atmos. Res. , 132, 91-101, 2013.

Lowe, D., Archer-Nicholls, S., Morgan, W., Allan, J., Utembe, S., Ouyang, B., Aruffo, E., Le Breton, M., Zaveri, R. A., and Di Carlo, P.: WRF-Chem model predictions of the regional impacts of N 2 O 5 heterogeneous processes on night-time chemistry over north-western Europe, Atmos. Chem. Phys., 15, 1385-1409, 2015.

Macintyre, H., and Evans, M.: Sensitivity of a global model to the uptake of N 2 O 5 by tropospheric aerosol, Atmos. Chem. Phys., 10, 7409-7414, 2010.

Martin, S. T.: Phase transitions of aqueous atmospheric particles, Chem. Rev., 100, 3403-3454, 2000.

McDuffie, E. E., Fibiger, D. L., Dubé, W. P., Lopez-Hilfiker, F., Lee, B. H., Thornton, J. A., Shah, V., Jaeglé, L., Guo, H., Weber, R. J., Michael Reeves, J., Weinheimer, A. J., Schroder, J. C., Campuzano-Jost, P., Jimenez, J. L., Dibb, J. E., Veres, P., Ebben, C., Sparks, T. L., Wooldridge, P. J., Cohen, R. C., Hornbrook, R. S., Apel, E. C., Campos, T., Hall, S. R., Ullmann, K., and Brown, S. S.: Heterogeneous N_2O_5 Uptake During Winter: Aircraft Measurements During the 2015 WINTER Campaign and Critical Evaluation of Current Parameterizations, J. Geophys. Res.: Atmos., 123, 4345-4372, 10.1002/2018jd028336, 2018.

McDuffie, E. E., Womack, C. C., Fibiger, D. L., Dube, W. P., Franchin, A., Middlebrook, A. M., Goldberger, L., Lee, B. H., Thornton, J. A., Moravek, A., Murphy, J. G., Baasandorj, M., and Brown, S. S.: On the contribution of nocturnal heterogeneous reactive nitrogen chemistry to particulate matter formation during wintertime pollution events in Northern Utah, Atmos. Chem. Phys., 19, 9287-9308, 10.5194/acp-19-9287-2019, 2019.

McNeill, V. F., Patterson, J., Wolfe, G. M., and Thornton, J. A.: The effect of varying levels of surfactant on the reactive uptake of N_2O_5 to aqueous aerosol, Atmos. Chem. Phys., 6, 1635-1644, 10.5194/acp-6-1635-2006, 2006.

Mentel, T. F., Sohn, M., and Wahner, A.: Nitrate effect in the heterogeneous hydrolysis of dinitrogen pentoxide on aqueous aerosols, PCCP, 1, 5451-5457, 10.1039/a905338g, 1999.

Mielke, L. H., Stutz, J., Tsai, C., Hurlock, S. C., Roberts, J. M., Veres, P. R., Froyd, K. D., Hayes, P. L., Cubison, M. J., Jimenez, J. L., Washenfelder, R. A., Young, C. J., Gilman, J. B., de Gouw, J. A., Flynn, J. H., Grossberg, N., Lefer, B. L., Liu, J., Weber, R. J., and Osthoff, H. D.: Heterogeneous formation of nitryl chloride and its role as a nocturnal NOx reservoir species during CalNex-LA 2010, J. Geophys. Res.: Atmos., 118, 10,638-610,652, 10.1002/jgrd.50783, 2013.

Mitroo, D., Gill, T. E., Haas, S., Pratt, K. A., and Gaston, C. J.: $CINO_2$ Production from N_2O_5 Uptake on Saline Playa Dusts: New Insights into Potential Inland Sources of $CINO_2$, Environmental Science & Technology, 53, 7442-7452, 10.1021/acs.est.9b01112, 2019.

Mozurkewich, M., and Calvert, J. G.: REACTION PROBABILITY OF N_2O_5 ON AQUEOUS AEROSOLS, J. Geophys. Res.- Atmos., 93, 15889-15896, 10.1029/JD093iD12p15889, 1988.

Murray, L. T., Fiore, A. M., Shindell, D. T., Naik, V., and Horowitz, L. W.: Large uncertainties in global hydroxyl projections tied to fate of reactive nitrogen and carbon, Proceedings of the National Academy of Sciences, 118, 2021.

Osthoff, H. D., Roberts, J. M., Ravishankara, A. R., Williams, E. J., Lerner, B. M., Sommariva, R., Bates, T. S., Coffman, D., Quinn, P. K., Dibb, J. E., Stark, H., Burkholder, J. B., Talukdar, R. K., Meagher, J., Fehsenfeld, F.

https://doi.org/10.5194/amt-2022-167
Preprint. Discussion started: 21 June 2022

C., and Brown, S. S.: High levels of nitryl chloride in the polluted subtropical marine boundary layer, Nat. Geosci. , 1, 324-328, 10.1038/ngeo177, 2008.

Phillips, G. J., Thieser, J., Tang, M., Sobanski, N., Schuster, G., Fachinger, J., Drewnick, F., Borrmann, S., Bingemer, H., Lelieveld, J., and Crowley, J. N.: Estimating N_2O_5 uptake coefficients using ambient measurements of NO_3, N_2O_5, $ClNO_2$ and particle-phase nitrate, Atmos. Chem. Phys., 16, 13231-13249, 10.5194/acp-16-13231-2016, 2016.

Platt, U. F., Winer, A. M., Biermann, H. W., Atkinson, R., and Pitts, J. N.: Measurement of nitrate radical concentrations in continental air, Environmental Science & Technology, 18, 365-369, 10.1021/es00123a015, 1984.

Prabhakar, G., Parworth, C. L., Zhang, X. L., Kim, H., Young, D. E., Beyersdorf, A. J., Ziemba, L. D., Nowak, J. B., Bertram, T. H., Faloona, I. C., Zhang, Q., and Cappa, C. D.: Observational assessment of the role of nocturnal residual-layer chemistry in determining daytime surface particulate nitrate concentrations, Atmos. Chem. Phys., 17, 14747-14770, 10.5194/acp-17-14747-2017, 2017.

Riedel, T. P., Bertram, T. H., Ryder, O. S., Liu, S., Day, D. A., Russell, L. M., Gaston, C. J., Prather, K. A., and Thornton, J. A.: Direct N_2O_5 reactivity measurements at a polluted coastal site, Atmos. Chem. Phys., 12, 2959-2968, 10.5194/acp-12-2959-2012, 2012.

Riemer, N., Vogel, H., Vogel, B., Schell, B., Ackermann, I., Kessler, C., and Hass, H.: Impact of the heterogeneous hydrolysis of N_2O_5 on chemistry and nitrate aerosol formation in the lower troposphere under photosmog conditions, J. Geophys. Res.- Atmos., 108, 10.1029/2002jd002436, 2003.

Riemer, N., Vogel, H., Vogel, B., Anttila, T., Kiendler-Scharr, A., and Mentel, T. F.: Relative importance of organic coatings for the heterogeneous hydrolysis of N_2O_5during summer in Europe, J. Geophys. Res. , 114, 10.1029/2008jd011369, 2009.

Sarwar, G., Simon, H., Bhave, P., and Yarwood, G.: Examining the impact of heterogeneous nitryl chloride production on air quality across the United States, Atmospheric Chemistry & Physics, 12, 6455-6473, 10.5194/acp-12-6455-2012, 2012.

Schweitzer, F., Mirabel, P., and George, C.: Multiphase chemistry of N_2O_5, $ClNO_2$, and $BrNO_2$, The Journal of Physical Chemistry A, 102, 3942-3952, 1998.

Tang, M., Telford, P., Pope, F. D., Rkiouak, L., Abraham, N., Archibald, A. T., Braesicke, P., Pyle, J., McGregor, J., and Watson, I.: Heterogeneous reaction of N 2 O 5 with airborne TiO 2 particles and its implication for stratospheric particle injection, Atmos. Chem. Phys., 14, 6035-6048, 2014.

Tham, Y. J., Wang, Z., Li, Q. Y., Yun, H., Wang, W. H., Wang, X. F., Xue, L. K., Lu, K. D., Ma, N., Bohn, B., Li, X., Kecorius, S., Gross, J., Shao, M., Wiedensohler, A., Zhang, Y. H., and Wang, T.: Significant concentrations of nitryl chloride sustained in the morning: investigations of the causes and impacts on ozone production in a polluted region of northern China, Atmos. Chem. Phys., 16, 14959-14977, 10.5194/acp-16-14959-2016, 2016.

Tham, Y. J., Wang, Z., Li, Q. Y., Wang, W. H., Wang, X. F., Lu, K. D., Ma, N., Yan, C., Kecorius, S., Wiedensohler, A., Zhang, Y. H., and Wang, T.: Heterogeneous N_2O_5 uptake coefficient and production yield of $ClNO_2$ in polluted northern China: roles of aerosol water content and chemical composition, Atmos. Chem. Phys., 18, 13155-13171, 10.5194/acp-18-13155-2018, 2018.

Thornton, J. A., Braban, C. F., and Abbatt, J. P. D.: N_2O_5 hydrolysis on sub-micron organic aerosols: the effect of relative humidity, particle phase, and particle size, PCCP, 5, 4593, 10.1039/b307498f, 2003.

Thornton, J. A., and Abbatt, J. P. D.: N_2O_5 reaction on submicron sea salt aerosol: Kinetics, products, and the effect of surface active organics, J. Phys. Chem. A, 109, 10004-10012, 10.1021/jp054183t, 2005.

https://doi.org/10.5194/amt-2022-167
Preprint. Discussion started: 21 June 2022

881 Thornton, J. A., Kercher, J. P., Riedel, T. P., Wagner, N. L., Cozic, J., Holloway, J. S., Dube, W. P., Wolfe, G. M.,
882 Quinn, P. K., Middlebrook, A. M., Alexander, B., and Brown, S. S.: A large atomic chlorine source inferred from
883 mid-continental reactive nitrogen chemistry, Nature, 464, 271-274, 10.1038/nature08905, 2010.
884 Van Doren, J. M., Watson, L. R., Davidovits, P., Worsnop, D. R., Zahniser, M. S., and Kolb, C. E.: Temperature
885 dependence of the uptake coefficients of nitric acid, hydrochloric acid and nitrogen oxide (N_2O_5) by water
886 droplets, J. Phys. Chem., 94, 3265-3269, 1990.
887 Wagner, N. L., Riedel, T. P., Young, C. J., Bahreini, R., Brock, C. A., Dubé, W. P., Kim, S., Middlebrook, A. M.,
888 Öztürk, F., Roberts, J. M., Russo, R., Sive, B., Swarthout, R., Thornton, J. A., VandenBoer, T. C., Zhou, Y., and
889 Brown, S. S.: N_2O_5 uptake coefficients and nocturnal NO_2 removal rates determined from ambient wintertime
890 measurements, J. Geophys. Res.: Atmos., 118, 9331-9350, 10.1002/jgrd.50653, 2013.
891 Wahner, A., Mentel, T. F., Sohn, M., and Stier, J.: Heterogeneous reaction of N_2O_5 on sodium nitrate aerosol, J.
892 Geophys. Res.: Atmos., 103, 31103-31112, 10.1029/1998jd100022, 1998.
893 Wang, H., Chen, J., and Lu, K.: Development of a portable cavity-enhanced absorption spectrometer for the
894 measurement of ambient NO₃ and
895 N₂O₅: experimental setup, lab characterizations, and field
896 applications in a polluted urban environment, Atmospheric Measurement Techniques, 10, 1465-1479,
897 10.5194/amt-10-1465-2017, 2017a.
898 Wang, H., Lu, K., Chen, X., Zhu, Q., Chen, Q., Guo, S., Jiang, M., Li, X., Shang, D., Tan, Z., Wu, Y., Wu, Z.,
899 Zou, Q., Zheng, Y., Zeng, L., Zhu, T., Hu, M., and Zhang, Y.: High N_2O_5 Concentrations Observed in Urban
900 Beijing: Implications of a Large Nitrate Formation Pathway, Environ Sci Tech Let, 4, 416-420,
901 10.1021/acs.estlett.7b00341, 2017b.
902 Wang, H., Chen, X., Lu, K., Tan, Z., Ma, X., Wu, Z., Li, X., Liu, Y., Shang, D., Wu, Y., Zeng, L., Hu, M., Schmitt,
903 S., Kiendler-Scharr, A., Wahner, A., and Zhang, Y.: Wintertime N_2O_5 uptake coefficients over the North China
904 Plain, Science Bulletin, 65, 765-774, https://doi.org/10.1016/j.scib.2020.02.006, 2020a.
905 Wang, H. C., Lu, K. D., Chen, X. R., Zhu, Q. D., Chen, Q., Guo, S., Jiang, M. Q., Li, X., Shang, D. J., Tan, Z. F.,
906 Wu, Y. S., Wu, Z. J., Zou, Q., Zheng, Y., Zeng, L. M., Zhu, T., Hu, M., and Zhang, Y. H.: High N_2O_5
907 Concentrations Observed in Urban Beijing: Implications of a Large Nitrate Formation Pathway, Environ Sci Tech
908 Let, 4, 416-420, 10.1021/acs.estlett.7b00341, 2017c.
909 Wang, H. C., Lu, K. D., Chen, X. R., Zhu, Q. D., Wu, Z. J., Wu, Y. S., and Sun, K.: Fast particulate nitrate
910 formation via N_2O_5 uptake aloft in winter in Beijing, Atmos. Chem. Phys., 18, 10483-10495, 10.5194/acp-18-
911 10483-2018, 2018a.
912 Wang, H. C., Lu, K. D., Guo, S., Wu, Z. J., Shang, D. J., Tan, Z. F., Wang, Y. J., Le Breton, M., Lou, S. R., Tang,
913 M. J., Wu, Y. S., Zhu, W. F., Zheng, J., Zeng, L. M., Hallquist, M., Hu, M., and Zhang, Y. H.: Efficient N_2O_5
914 uptake and NO_3 oxidation in the outflow of urban Beijing, Atmos. Chem. Phys., 18, 9705-9721, 10.5194/acp-18-
915 9705-2018, 2018b.
916 Wang, H. C., Chen, X. R., Lu, K. D., Hu, R. Z., Li, Z. Y., Wang, H. L., Ma, X. F., Yang, X. P., Chen, S. Y., Dong,
917 H. B., Liu, Y., Fang, X., Zeng, L. M., Hu, M., and Zhang, Y. H.: NO_3 and N_2O_5 chemistry at a suburban site
918 during the EXPLORE-YRD campaign in 2018, Atmos. Environ., 224, ARTN 117180
919 10.1016/j.atmosenv.2019.117180, 2020b.
920 Wang, H. C., Peng, C., Wang, X., Lou, S. R., Lu, K. D., Gan, G. C., Jia, X. H., Chen, X. R., Chen, J., Wang, H.
921 L., Fan, S. J., Wang, X. M., and Tang, M. J.: N_2O_5 uptake onto saline mineral dust: a potential missing source of
922 tropospheric $ClNO_2$ in inland China, Atmos. Chem. Phys., 22, 1845-1859, 10.5194/acp-22-1845-2022, 2022.

https://doi.org/10.5194/amt-2022-167
Preprint. Discussion started: 21 June 2022


Atmospheric Measurement Techniques Discussions

Wang, W., Wang, Z., Yu, C., Xia, M., Peng, X., Zhou, Y., Yue, D., Ou, Y., and Wang, T.: An in situ flow tube system for direct measurement of N_2O_5 heterogeneous uptake coefficients in polluted environments, Atmospheric Measurement Techniques, 11, 5643-5655, 10.5194/amt-11-5643-2018, 2018c.

Wang, X., Wang, H., Xue, L., Wang, T., Wang, L., Gu, R., Wang, W., Tham, Y. J., Wang, Z., Yang, L., Chen, J., and Wang, W.: Observations of N_2O_5 and $ClNO_2$ at a polluted urban surface site in North China: High N_2O_5 uptake coefficients and low $ClNO_2$ product yields, Atmos. Environ., 156, 125-134, 10.1016/j.atmosenv.2017.02.035, 2017d.

Wang, Y. L., Song, W., Yang, W., Sun, X. C., Tong, Y. D., Wang, X. M., Liu, C. Q., Bai, Z. P., and Liu, X. Y.: Influences of atmospheric pollution on the contributions of major oxidation pathways to PM2. 5 nitrate formation in Beijing, J. Geophys. Res.: Atmos., 124, 4174-4185, 2019.

Wang, Z., Wang, W., Tham, Y. J., Li, Q., Wang, H., Wen, L., Wang, X., and Wang, T.: Fast heterogeneous N_2O_5 uptake and $ClNO_2$ production in power plant and industrial plumes observed in the nocturnal residual layer over the North China Plain, Atmos. Chem. Phys., 17, 12361-12378, 10.5194/acp-17-12361-2017, 2017e.

Wang, Z., Wang, W. H., Tham, Y. J., Li, Q. Y., Wang, H., Wen, L., Wang, X. F., and Wang, T.: Fast heterogeneous N_2O_5 uptake and $ClNO_2$ production in power plant and industrial plumes observed in the nocturnal residual layer over the North China Plain, Atmos. Chem. Phys., 17, 12361-12378, 10.5194/acp-17-12361-2017, 2017f.

Wu, C., Zhang, S., Wang, G., Lv, S., Li, D., Liu, L., Li, J., Liu, S., Du, W., and Meng, J.: Efficient heterogeneous formation of ammonium nitrate on the saline mineral particle surface in the atmosphere of East Asia during dust storm periods, Environmental Science & Technology, 54, 15622-15630, 2020.

Xia, M., Wang, W., Wang, Z., Gao, J., Li, H., Liang, Y., Yu, C., Zhang, Y., Wang, P., Zhang, Y., Bi, F., Cheng, X., and Tao, W.: Heterogeneous Uptake of N_2O_5 in Sand Dust and Urban Aerosols Observed during the Dry Season in Beijing, Atmosphere, 10, 204, 10.3390/atmos10040204, 2019.

Yu, C., Wang, Z., Xia, M., Fu, X., Wang, W., Yee Jun, T., Chen, T., Zheng, P., Li, H., Shan, Y., Wang, X., Xue, L., Zhou, Y., Yue, D., Ou, Y., Gao, J., Lu, K., Brown, S., Zhang, Y., and Tao, W.: Heterogeneous N_2O_5 reactions on atmospheric aerosols at four Chinese sites: improving model representation of uptake parameters, Atmos. Chem. Phys., 20, 4367-4378, 10.5194/acp-20-4367-2020, 2020a.

Yu, C., Wang, Z., Xia, M., Fu, X., Wang, W. H., Tham, Y. J., Chen, T. S., Zheng, P. G., Li, H. Y., Shan, Y., Wang, X. F., Xue, L. K., Zhou, Y., Yue, D. L., Ou, Y. B., Gao, J., Lu, K. D., Brown, S. S., Zhang, Y. H., and Wang, T.: Heterogeneous N_2O_5 reactions on atmospheric aerosols at four Chinese sites: improving model representation of uptake parameters, Atmos. Chem. Phys., 20, 4367-4378, 10.5194/acp-20-4367-2020, 2020b.

Yun, H., Wang, T., Wang, W. H., Tham, Y. J., Li, Q. Y., Wang, Z., and Poon, S. C. N.: Nighttime NOx loss and $ClNO_2$ formation in the residual layer of a polluted region: Insights from field measurements and an iterative box model, Sci. Total Environ., 622, 727-734, 10.1016/j.scitotenv.2017.11.352, 2018.